Article

Synthesis and Characterization of Model Compounds of the Lysine Tyrosyl Quinone Cofactor of Lysyl Oxidase

Minae Mure, Sophie X. Wang, and Judith P. Klinman

J. Am. Chem. Soc., **2003**, 125 (20), 6113-6125• DOI: 10.1021/ja0214274 • Publication Date (Web): 29 April 2003

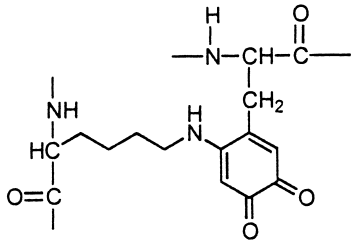

LTQ cofactor of Lysyl Oxidase

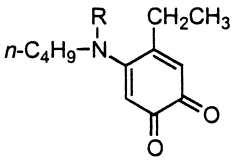

1_{ox}: R = H
3_{ox}: R = CH_3

Model compounds of LTQ cofactor

More About This Article

Additional resources and features associated with this article are available within the HTML version:

- Supporting Information
- Links to the 3 articles that cite this article, as of the time of this article download
- Access to high resolution figures
- Links to articles and content related to this article
- Copyright permission to reproduce figures and/or text from this article

View the Full Text HTML

J|A|C|S
ARTICLES
Published on Web 04/29/2003

Synthesis and Characterization of Model Compounds of the Lysine Tyrosyl Quinone Cofactor of Lysyl Oxidase

Minae Mure, Sophie X. Wang, and Judith P. Klinman*,†

Contribution from the Department of Chemistry, University of California, Berkeley, California 94720-1460

Received December 10, 2002; E-mail: klinman@socrates.berkeley.edu

Abstract: 4-*n*-Butylamino-5-ethyl-1,2-benzoquinone ($\mathbf{1}_{ox}$) has been synthesized as a model compound for the LTQ (lysine tyrosyl quinone) cofactor of lysyl oxidase (LOX). At pH 7, $\mathbf{1}_{ox}$ has a λ_{max} at 504 nm and exists as a neutral *o*-quinone in contrast to a TPQ (2,4,5-trihydroxyphenylalanine quinone) model compound, **4**, which is a resonance-stabilized monoanion. Despite these structural differences $\mathbf{1}_{ox}$ and **4** have the same redox potential (ca. −180 mV vs SCE). The structure of the phenylhydrazine adduct of $\mathbf{1}_{ox}$ (**2**) is reported, and 2D NMR spectroscopy has been used to show that the position of nucleophilic addition is at C_1. UV−vis spectroscopic pH titration of phenylhydrazine adducts of $\mathbf{1}_{ox}$ and **4**, **2**, and **11**, respectively, reveals a similar red shift in λ_{max} at alkaline pH with the same pK_a (∼11.8). In contrast, the red shift in λ_{max} at acidic pH conditions yields different pK_a values (2.12 for **2** vs −0.28 for **11**), providing a means to distinguish LTQ from TPQ. Reactions between in situ generated 4-ethyl-1,2-benzoquinone and primary amines give a mixture of products, indicating that the protein environment must play an essential role in LTQ biogenesis by directing the nucleophilic addition of the ϵ-amino group of a lysine residue to the C_4 position of a putative dopaquinone intermediate. Characterization of a 1,6-adduct between an *o*-quinone and butylamine (3-*n*-butylamino-5-ethyl-1,2-benzoquinone, **13**) confirms the assignment of LTQ as a 1,4-addition product.

Introduction

Lysyl oxidase (LOX; EC 1.4.3.13) is a copper-containing enzyme that plays an essential role in stabilizing extracellular matrices.[1−3] It catalyzes the oxidative deamination of the ϵ-amino group of peptidyl lysine in collagen and elastin, generating peptidyl α-aminoadipic-*δ*-semialdehyde. The peptidyl aldehyde then undergoes nonenzymatic condensation with either a neighboring aldehyde or an unmodified lysine side chain to form the intra- and intercovalent cross-linking of collagen and elastin. These molecules are deposited as insoluble fibers that provide strength and/or elasticity to connective tissues. Altered LOX activity has been associated with many disorders such as vascular rupture and torsion, loose skin and joints, and fibrotic diseases.[3−5] Assays in vitro have shown that LOX can also oxidatively deaminate a variety of aliphatic monoamines and diamines, synthetic elastin-like polypeptides, and lysine in histone H1 and other proteins.[6,7] Recently, increasing numbers of publications have suggested that LOX may possess alternative functions such as developmental regulation,[8] tumor suppression,[9−13] cell growth control,[14,15] and cell adhesion.[16,17] While the physiological role of LOX has been well studied, its structure has not been solved, and the catalytic mechanism is not fully characterized.

LOX has been classified as a copper amine oxidase (CAO; EC 1.4.3.6), but it is distinguished from other CAOs by having a monomeric structure (32 kDa), whereas the CAOs are homodimers (75−80 kDa per monomer).[18−22] Analogous to other CAOs, LOX is believed to contain an organic cofactor and one copper(II) at its active site.[23,24] The nature of the organic

† J.P.K. is also with the Department of Molecular and Cell Biology, University of California, Berkeley, CA 94720-1460.

(1) Csiszar, K. *Prog. Nucleic Acid Res. Mol. Biol.* **2001**, *70*, 1−32.
(2) Rucker, R. B.; Kosonen, T.; Clegg, M. S.; Mitchell, A. E.; Rucker, B. R.; UriuHare, J. Y.; Keen, C. L. *Am. J. Clin. Nutr.* **1998**, *67*, S996−S1002.
(3) SmithMungo, L. I.; Kagan, H. M. *Matrix Biol.* **1998**, *16*, 387−398.
(4) Kagan, H. M. *Pathol. Res. Pract.* **1994**, *190*, 910−919.
(5) Streichenberger, N.; Peyrol, S.; Philit, F.; Loire, R.; Sommer, P.; Cordier, J. F. *Virchows. Arch.* **2001**, *439*, 78−84.
(6) Kagan, H. M.; Williams, M. A.; Williamson, P. R.; Anderson, J. M. *J. Biol. Chem.* **1984**, *259*, 11203−11207.
(7) Ohkawa, K.; Fujii, K.; Nishida, A.; Yamauchi, T.; Ishibashi, H.; Yamamoto, H. *Biomacromolecules* **2001**, *2*, 773−779.
(8) Butler, E.; Handlin, J.; Benson, S. *Exp. Cell Res.* **1987**, *173*, 174−182.
(9) Kenyon, K.; Contente, S.; Trackman, P. C.; Tang, J.; Kagan, H. M.; Friedman, R. M. *Science* **1991**, *253*, 802.
(10) Hajnal, A.; Klemenz, R.; Schafer, R. *Cancer Res.* **1993**, *53*, 4670−4675.
(11) Oberhuber, H.; Seliger, B.; Schafer, R. *Mol. Carcinog.* **1995**, *12*, 198−204.
(12) Peyrol, S.; Raccurt, M.; Gerard, F.; Gleyzal, C.; Grimaud, J. A.; Sommer, P. *Am. J. Pathol.* **1997**, *150*, 497−507.
(13) Ren, C. Z.; Yang, G.; Timme, T. L.; Wheeler, T. M.; Thompson, T. C. *Cancer Res.* **1998**, *58*, 1285−1290.
(14) Csiszar, K.; Entersz, I.; Trackman, P. C.; Samid, D.; Boyd, C. D. *Mol. Biol. Rep.* **1996**, *23*, 97−108.
(15) Li, W. D.; Liu, G. M.; Chou, I. N.; Kagan, H. M. *J. Cell. Biochem.* **2000**, *78*, 550−557.
(16) Ito, H.; Akiyama, H.; Iguchi, H.; Iyama, K.; Miyamoto, M.; Ohsawa, K.; Nakamura, T. *J. Biol. Chem.* **2001**, *276*, 24023−24029.
(17) Omori, K.; Fujiseki, Y.; Suzukawa, J.; Inagaki, C. *Matrix Biol.* **2002**, *21*, 337−348.
(18) McIntire, W. S.; Hartmann, C. In *Principles and applications of quinoproteins*; Davidson, V. L., Ed.; Dekker: New York, 1993; pp 97−171.
(19) Knowles, P. F.; Dooley, D. M. In *Metal ions in biological systems*; Sigel, H., Sigel, A., Eds.; Dekker: New York, 1994; Vol. 30, pp 360−403.
(20) Klinman, J. P.; Mu, D. *Annu. Rev. Biochem.* **1994**, *63*, 299−344.
(21) Jalkanen, S.; Salmi, M. *EMBO J.* **2001**, *20*, 3893−3901.
(22) Mure, M.; Mills, S. A.; Klinman, J. P. *Biochemistry* **2002**, *41*, 9269−9278.

cofactor has been controversial and was once thought to be pyrroloquinoline quinone (PQQ).[25] In 1996, following the discovery of a new quinonoid cofactor, topaquinone (TPQ) of a CAO,[26] lysine tyrosylquinone (LTQ) was identified as the cofactor of LOX.[27] LTQ is a new variant of the quinonoid cofactor and derives from cross-linking of a modified tyrosine with a lysine residue within the same polypeptide chain. There are two other identified cross-linked quinonoid cofactors, namely, tryptophan tryptophylquinone (TTQ)[28] and cysteine tryptophylquinone (CTQ) in bacterial amine dehydrogenases.[29−31] Among the quinonoid cofactors, TPQ has been the most extensively studied.[20,22,32] TPQ has been shown to form from a tyrosine residue by a self-catalytic process that requires only copper and dioxygen; a presumed intermediate is dopaquinone, which can undergo attack by hydroxide ion to yield the mature cofactor.[32−35] A number of compounds that model TPQ have been synthesized, and their ability to catalyze the oxidative deamination of primary amines was examined.[36−42] Further, TPQ derivatives that mimic both the proposed reaction intermediates and products of CAOs with substrate amines and inhibitors have been prepared and characterized with regard to their spectroscopic and redox properties.[37−39] These solution studies of TPQ model compounds and their derivatives have played an important role in helping to understand the mechanism of enzymatic reaction (see Chart 1).

It has been proposed that nucleophilic addition of the ϵ-amino group of a lysine residue to the dopaquinone intermediate, derived from a tyrosine residue as proposed in TPQ biogenesis, yields LTQ.[27] Analogous cross-linking of a modified tyrosine with glutathione or histidine has been observed in insects.[43−45] Further, such chemistry has been implicated in Lewy body formation (neuronal inclusions)[46] and also in degeneration of dopaminergic neurons[47] where both processes are proposed to be related to Parkinson's disease. To date, detailed investigations of the mechanism of LTQ formation in LOX have been limited by the lack of a suitable in vitro overexpression system.

Chart 1. Structures of Quinonoid Cofactors

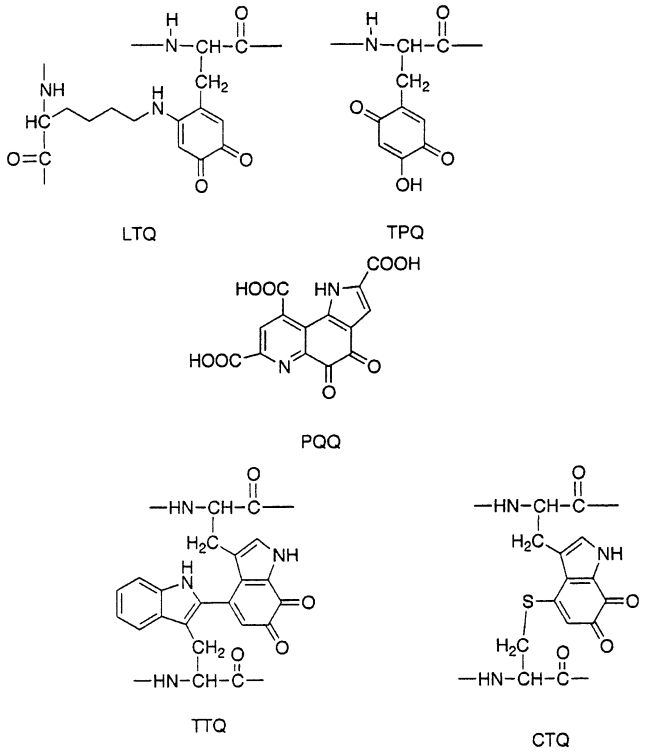

To fully understand the mechanism of LTQ formation in and subsequent to catalysis by LOX, it is important to characterize the basic chemical and physiological properties of LTQ. We have used the compound 4-*n*-butylamino-5-ethyl-1,2-benzoquinone ($\mathbf{1}_{ox}$) as a model of LTQ.[27,48] The structure of LTQ in LOX was first elucidated by comparison of the spectroscopic properties between the phenylhydrazine adduct of enzyme and the phenylhydrazine derivative of $\mathbf{1}_{ox}$ (**2**).[27] A subsequent study showed that resonance Raman spectra of underivatized LOX were in excellent agreement with that of $\mathbf{1}_{ox}$.[48] Recent studies of LTQ model compounds focused on their reactivity toward amines and decomposition during the catalytic turnover reaction.[49,50] However, there has been no systematic characterization of the spectroscopic, acid−base, and electrochemical properties of any LTQ model compound as they relate to the cofactor in LOX.

In this paper, we describe the syntheses of $\mathbf{1}_{ox}$, its reduced form $\mathbf{1}_{red}$, and its N-alkylated derivative ($\mathbf{3}_{ox}$) and compare their spectroscopic and redox properties with TPQ model compounds (**4**, **5**) and other quinones (**6**−**9**). The acid−base properties of the phenylhydrazone (**2**) and the analogous 4-nitrophenylhydrazine derivative (**10**) are studied and compared with those of the corresponding adducts of TPQ (**11**, **12**). In relation to LTQ

(23) Gacheru, S. N.; Trackman, P. C.; Shah, M. A.; Ogara, C. Y.; Spacciapoli, P.; Greenaway, F. T.; Kagan, H. M. *J. Biol. Chem.* **1990**, *265*, 19022−19027.
(24) Iguchi, H.; Sano, S. *Connect. Tissue Res.* **1985**, *14*, 129−139.
(25) Williamson, P. R.; Moog, R. S.; Dooley, D. M.; Kagan, H. M. *J. Biol. Chem.* **1986**, *261*, 16302−16305.
(26) Janes, S. M.; Mu, D.; Wemmer, D.; Smith, A. J.; Kaur, S.; Maltby, D.; Burlingame, A. L.; Klinman, J. P. *Science* **1990**, *248*, 981−987.
(27) Wang, S. X.; Mure, M.; Medzihradszky, K. F.; Burlingame, A. L.; Brown, D. E.; Dooley, D. M.; Smith, A. J.; Kagan, H. M.; Klinman, J. P. *Science* **1996**, *273*, 1078−1084.
(28) McIntire, W. S.; Wemmer, D. E.; Chistoserdov, A.; Lidstrom, M. E. *Science* **1991**, *252*, 817−824.
(29) Datta, S.; Mori, Y.; Takagi, K.; Kawaguchi, K.; Chen, Z. W.; Okajima, T.; Kuroda, S.; Ikeda, T.; Kano, K.; Tanizawa, K.; Mathews, F. S. *Proc. Natl. Acad. Sci. U.S.A.* **2001**, *98*, 14268−14273.
(30) Vandenberghe, I.; Kim, J. K.; Devreese, B.; Hacisalihoglu, A.; Iwabuki, H.; Okajima, T.; Kuroda, S.; Adachi, O.; Jongejan, J. A.; Duine, J. A.; Tanizawa, K.; Van Beeumen, J. *J. Biol. Chem.* **2001**, *276*, 42923−42931.
(31) Satoh, A.; Kim, J. K.; Miyahara, I.; Devreese, B.; Vandenberghe, I.; Hacisalihoglu, A.; Okajima, T.; Kuroda, S.; Adachi, O.; Duine, J. A.; Van Beeumen, J.; Tanizawa, K.; Hirotsu, K. *J. Biol. Chem.* **2002**, *277*, 2830−2834.
(32) Schwartz, B.; Klinman, J. P. *Vitam. Horm.* **2001**, *61*, 219−239.
(33) Klinman, J. P. *J. Biol. Chem.* **1996**, *271*, 27189−27192.
(34) Dooley, D. M. *J. Biol. Inorg. Chem.* **1999**, *4*, 1−11.
(35) Kim, M.; Okajima, T.; Kishishita, S.; Yoshimura, M.; Kawamori, A.; Tanizawa, K.; Yamaguchi, H. *Nat. Struct. Biol.* **2002**, *9*, 591−596.
(36) Mure, M.; Klinman, J. P. *J. Am. Chem. Soc.* **1993**, *115*, 7117−7127.
(37) Mure, M.; Klinman, J. P. *J. Am. Chem. Soc.* **1995**, *117*, 8698−8706.
(38) Mure, M.; Klinman, J. P. *J. Am. Chem. Soc.* **1995**, *117*, 8707−8718.
(39) Mure, M.; Klinman, J. P. *Methods Enzymol.* **1995**, *258*, 39−52.
(40) Lee, Y.; Sayre, L. M. *J. Am. Chem. Soc.* **1995**, *117*, 11823−11828.
(41) Lee, Y. H.; Sayre, L. M. *J. Am. Chem. Soc.* **1995**, *117*, 3096−3105.
(42) Lee, Y. H.; Huang, H.; Sayre, L. M. *J. Am. Chem. Soc.* **1996**, *118*, 7241−7242.
(43) Leem, J. Y.; Nishimura, C.; Kurata, S.; Shimada, I.; Kobayashi, A.; Natori, S. *J. Biol. Chem.* **1996**, *271*, 13573−13577.
(44) Xu, R. D.; Huang, X.; Hopkins, T. L.; Kramer, K. J. *Insect Biochem. Mol. Biol.* **1997**, *27*, 101−108.
(45) Kramer, K. J.; Kanost, M. R.; Hopkins, T. L.; Jiang, H. B.; Zhu, Y. C.; Xu, R. D.; Kerwin, J. L.; Turecek, F. *Tetrahedron* **2001**, *57*, 385−392.
(46) Montine, T. J.; Farris, D. B.; Graham, D. G. *J. Neuropathol. Exp. Neurol.* **1995**, *54*, 311−319.
(47) Hastings, T. G.; Zigmond, M. J. *J. Neurochem.* **1994**, *63*, 1126−1132.
(48) Wang, S. X.; Nakamura, N.; Mure, M.; Klinman, J. P.; SandersLoehr, J. *J. Biol. Chem.* **1997**, *272*, 28841−28844.
(49) Ling, K. Q.; Kim, J.; Sayre, L. M. *J. Am. Chem. Soc.* **2001**, *123*, 9606−9611.
(50) Akagawa, M.; Suyama, K. *Biochem. Biophys. Res. Commun.* **2001**, *281*, 193−199.

Chart 2

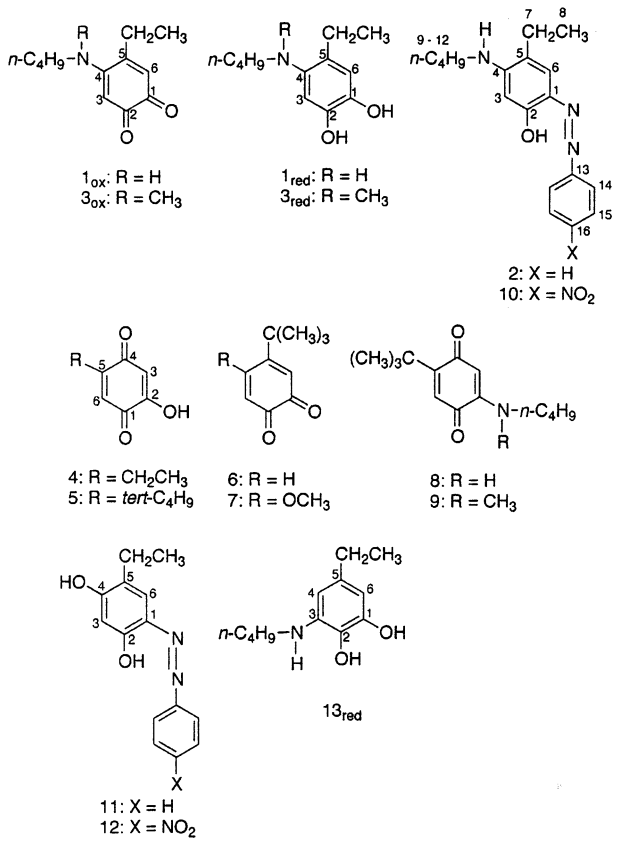

biogenesis, we report preliminary findings involving the oxidation of 3-*n*-butylamino-5-ethylcatechol (**13**$_{red}$) and the reaction of 4-ethylphenol and *N*-methyl-*n*-butylamine catalyzed by a mushroom tyrosinase. These studies provide support for the proposed 1,4-addition of lysine to an *o*-quinone intermediate during LTQ production (see Chart 2).

Experimental Section

Materials. 6-Nitropiperonal, 5-nitrovanillin, and *N*-methyl-*n*-butylamine were purchased from Aldrich. 4-Ethylcatechol was purchased from Lancaster. 2-Hydroxy-5-ethyl-1,4-benzoquinone (**4**), 2-hydroxy-5-*tert*-butyl-1,4-benzoquinone (**5**), 4-*tert*-butyl-1,2-benzoquinone (**6**), and 4-methoxy-5-*tert*-butyl-1,2-benzoquinone (**7**) were prepared according to the methods described previously.[37] Mushroom tyrosinase (EC 1.14.18.1) was purchased from Sigma.

Methods. UV−vis absorbance data were obtained on a HP8452A diode array spectrophotometer equipped with a thermostated cell holder at 25 ± 0.2 °C (path length of 1 cm). Mass spectra (MS) were obtained on a VG 70-SE or a VG ZAB 2-EQ instrument.

(A) Synthesis of 4,5-(Methylenedioxy)-2-nitrostyrene. Anhydrous methyltriphenylphosphonium bromide (37 g, 103 mmol) was suspended in anhydrous THF (500 mL) in a 1 L round-bottomed flask under an atmosphere of dry N_2. The flask was cooled on ice prior to addition of an equimolar amount of sodium bis(trimethylsilyl)amide (1 M in THF, 103 mL), and the mixture was stirred at room temperature under N_2 for 1 h. Then 6-nitropiperonal (15.33 g, 77 mmol) was added in one portion under N_2, and the reaction mixture was stirred at room temperature for a further 5 h. The solvent was removed by rotary evaporation, and the resulting residue was diluted with water and extracted with ethyl acetate. The combined organic layer was washed with saturated aqueous NaCl and dried over $MgSO_4$, and the solvent was removed under reduced pressure. The resulting crude product was purified by silica gel chromatography (eluent: hexanes:ethyl acetate = 20/1 v/v) to yield 10.26 g (69% yield) of 4,5-(methylenedioxy)-2-nitrostyrene as a light yellow solid: ^{1}H NMR ($CDCl_3$) δ 5.404 (1H, d, J = 10.9 Hz, −CH=C**H**$_2$ cis), 5.610 (1H, dd, J = 0.5, 17.0 Hz, −CH=C**H**$_2$ trans and geminal), 6.098 (2H, −OC**H**$_2$O−), 6.971 (1H, s, ring proton at C_6), 7.187 (1H, dd, J = 10.9, 17.2 Hz, −C**H**=CH$_2$), 7.466 (1H, s, ring proton at C_3).

(B) Synthesis of 2-Ethyl-4,5-methylenedioxyaniline. The reduction of 4,5-(methylenedioxy)-2-nitrostyrene was performed according to the reported method[51] with some modifications. $NaBH_4$ (0.95 g, 25 mmol) was added to a yellow solution of 4,5-(methylenedioxy)-2-nitrostyrene (2.62 g, 13.6 mmol) in THF (50 mL). Palladium on carbon (10%, 0.4 g) was added in one portion, and the mixture was stirred at room temperature for 30 min. At this point, the reduction was incomplete as determined by TLC. Acidification by dropwise addition of 2 N HCl caused bleaching of the reaction mixture, indicating the completion of the reduction, which was confirmed by TLC. The catalyst was removed by filtration, and the filtrate was extracted three times with ethyl acetate. Then the pH of the aqueous layer was adjusted to >10 by addition of 10 N NaOH and then extracted five times with ethyl acetate. The combined ethyl acetate layers were dried over $MgSO_4$, and the solvent was removed under reduced pressure to yield 2.13 g (95%) of 2-ethyl-4,5-methylenedioxyaniline as a slightly discolored oil. Prolonged drying under vacuum yielded opaque needles: ^{1}H NMR ($CDCl_3$) δ 1.206 (3H, t, J = 7.5 Hz, −CH$_2$C**H**$_3$), 2.436 (2H, q, J = 7.5 Hz, −C**H**$_2$CH$_3$), 3.430 (2H, br s, exchangeable, −NH), 5.829 (2H, s, −OC**H**$_2$O−), 6.290 (1H, s, ring proton at C_6), 6.604 (1H, s, ring proton at C_3).

(C) Synthesis of *N*-*n*-Butyl-2-ethyl-4,5-methylenedioxyaniline. 4,5-(Methylenedioxy)-2-nitrostyrene (1.93 g, 11.7 mmol) in anhydrous THF (120 mL) was treated with molar equivalents of *n*-butyllithium (1.6 M in hexane, 7.3 mL) and *n*-butyl bromide (1.26 mL) while being cooled in an ice bath under an atmosphere of dry N_2. 1,4-Dioxane (10.5 mmol, 0.89 mL, dehydrated by treating with 4 Å molecular sieves previously dried at 300 °C) was then added, and the mixture was heated to 60 °C for 2 h. The solvent was removed by evaporation under reduced pressure, and the crude product was purified by silica gel chromatography (eluent: hexanes/ethyl acetate = 20/1 v/v) to give 2.07 g (80%) of *N*-*n*-butyl-2-ethyl-4,5-ethylenedioxyaniline as opaque needles: ^{1}H NMR ($CDCl_3$) δ 0.970 [3H, t, J = 7.4 Hz, −NH(CH$_2$)$_3$C**H**$_3$], 1.205 (3H, t, J = 7.5 Hz, −CH$_2$C**H**$_3$), 1.450 [2H, m, −NH(CH$_2$)$_2$C**H**$_2$CH$_3$], 1.628 (2H, m, −NHCH$_2$C**H**$_2$CH$_2$CH$_3$), 2.410 (2H, q, J = 7.5 Hz, −C**H**$_2$CH$_3$), 3.086 [2H, t, J = 7.1 Hz, −NHC**H**$_2$(CH$_2$)$_2$CH$_3$], 3.3 (1H, br s, exchangeable, −NH−), 5.827 (2H, s, −OC**H**$_2$O−), 6.318 (1H, s, 6-H), 6.632 (1H, s, 3-H); MS (EI) *m*/*z* 211.1 (M$^+$); HRMS (EI) $C_{12}H_{19}NO_2$ (M$^+$ − HCl) calcd 221.14158, obsd 221.14152.

(D) Synthesis of 4-*n*-Butylamino-5-ethyl-1,2-dihydroxybenzene (1$_{red}$). *N*-*n*-Butyl-2-ethyl-4,5-ethylenedioxyaniline (0.22 g, 1 mmol) in dichloromethane (25 mL) was stirred at room temperature under an atmosphere of deoxygenated Ar for 30 min. Boron trichloride (1 M in dichloromethane, 5 mL) was added to the mixture, which was then stirred at room temperature under Ar for 1.5 h. The reaction was quenched by addition of methanol (10 mL) which had been deoxygenated with Ar. The solvent was removed in vacuo, and the residue was redissolved in degassed methanol (5 mL). The methanol solution was heated under reflux for 5 min, and again the solvent was removed in vacuo. This operation was repeated three times to give a hydrochloride salt of 4-*n*-butylamino-5-ethyl-1,2-dihydroxybenzene (**1**$_{red}$) as a slightly discolored oil which formed into opaque needles in vacuo (quantitative yield): ^{1}H NMR (CD_3CN) δ 0.831 [3H, t, J = 7.4 Hz, −NH(CH$_2$)$_3$C**H**$_3$], 1.182 (3H, t, J = 7.4 Hz, −CH$_2$C**H**$_3$), 1.327 [2H, sextet, J = 7.4 Hz, −NH(CH$_2$)$_2$C**H**$_2$CH$_3$], 1.749 (2H, tt, J = 7.4, 7.9 Hz, −NHCH$_2$C**H**$_2$CH$_2$CH$_3$), 2.249 (br s, exchangeable, N**H**CH$_2$CH$_2$CH$_2$CH$_3$), 2.636 (2H, q, J = 7.4 Hz, −C**H**$_2$CH$_3$), 3.158 (2H, t, J = 7.9 Hz, −NHC**H**$_2$CH$_2$CH$_2$CH$_3$), 6.761 (1H, s, 3-H), 7.118 (1H, br s, exchangeable, −OH), 7.209 (1H, s, 6-H), 8.272 (1H, br s, exchangeable,

(51) Vitale, A. A.; Chiocconi, A. A. *J. Chem. Res., Suppl.* **1996**, 336−337.

−OH), 10.229 (2H, br s, exchangeable); ^{13}C NMR (CD_3CN) δ 12.8, 15.3, 19.2, 23.2, 26.8, 47.3, 59.5, 108.2, 117.0, 128.9, 129.2, 144.8, 146.4; MS (EI) *m*/*z* 209 (M^+ − HCl, 56%), 166 (M^+ − HCl − $C_3H_7^+$, 100%); HRMS (EI) $C_{12}H_{19}NO_2$ (M^+ − HCl) calcd 209.14158, obsd 209.14132.

(E) Synthesis of 4-*n*-Butylamino-5-ethyl-1,2-benzoquinone ($\mathbf{1}_{ox}$). $\mathbf{1}_{red}$ (22.5 mg, 0.09 mmol) was dissolved in a CH_3CN-H_2O solution (1:4, 10 mL), and a 10 μL aliquot of NaOH (1 M) was added to the mixture to facilitate the autoxidation. The reaction was monitored by UV−vis spectroscopy (formation of a species absorbing at 504 nm), and when the oxidation was complete, the reaction mixture was frozen in liquid N_2. The solvent was removed by lyophilization to yield $\mathbf{1}_{ox}$ as a dark purple solid (quantitative yield): ^{1}H NMR (CD_3CN) δ 0.947 [3H, t, J = 7.4 Hz, −NH(CH$_2$)$_3$C**H**$_3$], 1.167 (3H, t, J = 7.3 Hz, −CH$_2$C**H**$_3$), 1.395 [2H, m, −NH(CH$_2$)$_2$C**H**$_2$CH$_3$], 1.640 (2H, m, −NHCH$_2$C**H**$_2$CH$_2$CH$_3$), 2.485 (2H, dq, J = 1.5, 7.3 Hz, −C**H**$_2$CH$_3$), 3.270 (2H, m, −NHC**H**$_2$CH$_2$CH$_2$CH$_3$), 5.410 (1H, s, 3-H), 6.154 (1H, t, J = 1.5 Hz, 6-H), 6.226 (1H, br s, −NH); MS (EI) *m*/*z* 207 (M^+, 73%), 150 (M^+ − $C_4H_9^+$, 100%); HRMS (EI) $C_{12}H_{17}NO_2$ (M^+) calcd 207.12593, obsd 207.12559.

(F) Synthesis of *N*-*n*-Butyl-*N*-methyl-2-ethyl-4,5-methylenedioxyaniline. Aqueous formaldehyde (37%, 2 mL) was added to an ice-cold mixture of *N*-*n*-butyl-2-ethyl-4,5-methylenedioxyaniline (108.1 mg, 0.49 mmol) and formic acid (2 mL). The reaction mixture was stirred overnight at 90 °C and then cooled to room temperature. Concentrated HCl (2 mL) was added, and an extraction was performed with diethyl ether. The aqueous layer was treated with 50% NaOH to adjust the pH to 10 and then reextracted with diethyl ether. The combined ether layers were washed with water and dried over Na_2SO_4. The solvent was removed under reduced pressure to give *N*-*n*-butyl-*N*-methyl-2-ethyl-4,5-methylenedioxyaniline as a yellow oil (55% yield): ^{1}H NMR ($CDCl_3$) δ 0.888 [3H, t, J = 7.2 Hz, −N(CH$_3$)(CH$_2$)$_3$C**H**$_3$], 1.167 (3H, t, J = 7.6 Hz, −CH$_2$C**H**$_3$), 1.312 [2H, m, −N(CH$_3$)(CH$_2$)$_2$C**H**$_2$CH$_3$], 1.395 [2H, m, −N(CH$_3$)CH$_2$C**H**$_2$CH$_2$CH$_3$], 2.549 [3H, s, −N(C**H**$_3$)(CH$_2$)$_3$CH$_3$], 2.657 (2H, q, J = 7.6 Hz, −C**H**$_2$CH$_3$), 2.743 [2H, t, J = 7.5 Hz, −N(CH$_3$)C**H**$_2$(CH$_2$)$_2$CH$_3$], 5.890 (2H, s, −OC**H**$_2$O−), 6.701 (1H, s, ring proton at C_6), 6.710 (1H, s, ring proton at C_3).

(G) Synthesis of *N*-*n*-Butyl-*N*-methylamino-5-ethyl-1,2-dihydroxybenzene ($\mathbf{3}_{red}$) and 4-(*N*-*n*-Butyl-*N*-methylamino)-5-ethyl-1,2-benzoquinone ($\mathbf{3}_{ox}$). A solution of *N*-*n*-butyl-*N*-methyl-2-ethyl-4,5-methylenedioxyaniline (63.6 mg, 0.27 mmol) in dichloromethane was stirred at room temperature for 30 min under Ar and treated with boron trichloride (1 M in dichloromethane, 1.4 mL). The mixture was then stirred under Ar at room temperature for a further 3 h. The reaction was quenched by addition of methanol (5 mL), and the resulting solution was heated under reflux for 5 min after which time the solvent was removed in vacuo. The hydrochloride salt of *N*-*n*-butyl-*N*-methylamino-5-ethyl-1,2-dihydroxybenzene was isolated as a yellow-brown solid in quantitative yield. The compound is pure as indicated by ^{13}C NMR and mass spectrometry. The ^{1}H NMR in CD_3CN indicated that $\mathbf{3}_{red}$ is present as a mixture of two forms. The chemical shifts and integrations of the methylene protons of the *n*-butyl side chain [CH$_3$CH$_2$C**H**$_2$C**H**$_2$N(C**H**$_3$)−], the methyl protons [CH$_3$CH$_2$CH$_2$CH$_2$N(C**H**$_3$)−], and the methylene protons of the ethyl side chain suggest that there are two inequivalent forms of each. The resonances for the remaining protons are equivalent for the two forms. This could result from $\mathbf{3}_{red}$ existing as a mixture of the protonated and neutral forms in CD_3CN, or the *R* and *S* forms of $\mathbf{3}_{red}$ (where the protonated amine is the chiral center) may form hydrogen-bonded dimers in CD_3CN, thereby creating the diastereomers. In contrast to ^{1}H NMR, the ^{13}C NMR in this solvent can be assigned to a single species, $\mathbf{3}_{red}$: ^{1}H NMR (CD_3CN) δ 0.763 [3H, t, J = 7.2 Hz, −N(CH$_3$)(CH$_2$)$_3$C**H**$_3$], 1.122 (3H, t, J = 7.6 Hz, −CH$_2$C**H**$_3$), 1.20−1.23 [3H, m, −N(CH$_3$)CH$_2$C**H**$_2$C**H**$_2$CH$_3$], 1.563 [1H, m, −N(CH$_3$)CH$_2$C**H**$_2$CH$_2$CH$_3$], 2.710 (1H, 2q, J = 7.6 Hz, −C**H**$_2$CH$_3$), 2.821 (1H, 2q, J = 7.6 Hz, −C**H**$_2$CH$_3$), 3.090 [1.5H, s, −N(C**H**$_3$)(CH$_2$)$_3$CH$_3$], 3.102 [1.5H, s, −N(C**H**$_3$)(CH$_2$)$_3$CH$_3$], 3.423 [2H, br m, −N(CH$_3$)C**H**$_2$(CH$_2$)$_2$CH$_3$], 6.869 (1H, s, ring proton at C_3), 7.071 (1H, s, ring proton at C_6), ∼8.5 (br s, −OH), 10.10 (br s, −OH); ^{13}C NMR (CD_3CN) δ 12.8, 15.3, 19.2, 23.2, 29.8, 47.3, 59.5, 108.2, 117.0, 128.9, 129.2, 131.7, 144.8, 146.4; MS (EI) *m*/*z* 223 (M^+, 34%), 180 (M^+ − $C_3H_7^+$, 100%); HRMS (EI) $C_{13}H_{21}NO_2$ (M^+) calcd 223.15723, obsd 223.15703.

4-(*N*-*n*-butyl-*N*-methylamino)-5-ethyl-1,2-benzoquinone ($\mathbf{3}_{ox}$) was generated in situ by autoxidation of *N*-*n*-butyl-*N*-methylamino-5-ethyl-1,2-dihydroxybenzene as described in the synthesis of the quinone ($\mathbf{1}_{ox}$). $\mathbf{3}_{ox}$ was stable in a dilute aqueous solution but decomposed upon either solvent removal by lyophilization or when concentrated, thereby preventing full characterization. Attempts to extract $\mathbf{3}_{ox}$ with organic solvents were unsuccessful due to the instability of the quinone.

(H) Synthesis of 2-*N*-*n*-Butylamino-5-*tert*-butyl-1,4-benzoquinone (8) and 2-(*N*-*n*-Butyl-*N*-methylamino)-5-*tert*-butyl-1,4-benzoquinone (9). 8 and **9** were formed from the reactions of 2-*tert*-butyl-1,4-benzoquinone and *n*-butylamine and *N*-methyl-*n*-butylamine, respectively, and then purified by silica gel chromatography. The reaction conditions were same as described for the reaction of 2-*tert*-butyl-1,4-benzoquinone and benzylamine.[37] **8**: ^{1}H NMR ($CDCl_3$) δ 0.946 [3H, t, J = 7.3 Hz, −NH(CH$_2$)$_3$C**H**$_3$], 1.296 [9H, s, −(C**H**$_3$)$_3$], 1.396 [2H, m, −N-(CH$_2$)$_2$C**H**$_2$CH$_3$], 1.611 (2H, m, −NHCH$_2$C**H**$_2$CH$_2$CH$_3$), 3.062 [2H, 2t, −NHC**H**$_2$(CH$_2$)CH$_3$], 5.382 (1H, s, ring proton at C_3 + 1H, br s, NH), 6.425 (1H, s, ring proton at C_6); ^{13}C NMR ($CDCl_3$) δ 13.6, 20.0, 29.6, 30.1, 35.6, 41.9, 100.1, 127.2, 134.8, 145.3, 184.7, 185.6. **9**: ^{1}H NMR ($CDCl_3$) δ 0.936 [3H, t, J = 7.3 Hz, −NH(CH$_2$)$_3$C**H**$_3$], 1.277 [9H, s, −(C**H**$_3$)$_3$], 1.396 [2H, m, −N-(CH$_2$)$_2$C**H**$_2$CH$_3$], 1.578 [2H, m, −N(CH$_3$)CH$_2$C**H**$_2$CH$_2$CH$_3$], 2.982 [3H, s, −N(C**H**$_3$)(CH$_2$)$_3$CH$_3$], 3.477 [2H, 2t, −N(CH$_3$)C**H**$_2$(CH$_2$)CH$_3$], 5.478 (1H, s, ring proton at C_3), 6.303 (1H, s, ring proton at C_6); ^{13}C NMR ($CDCl_3$) δ 13.8, 20.0, 29.5, 29.9, 35.0, 40.1, 53.7, 106.1, 129.6, 148.9, 156.8, 185.5, 186.5.

(I) Synthesis of a Phenylhydrazine Adduct of $\mathbf{1}_{ox}$ (2). To a heated stirred solution of phenylhydrazine hydrochloride (70.1 mg, 0.485 mmol) in glacial acetic acid (5 mL) at 100 °C was added an acetic acid solution (2 mL) of $\mathbf{1}_{ox}$ (18.6 mg, 0.09 mmol). The reaction mixture was stirred at 100 °C for 30 min and then cooled to room temperature. Water (50 mL) was added, and the mixture was neutralized by $NaHCO_3$ and extracted with diethyl ether. The combined organic layers were washed with water and dried with $MgSO_4$, and the solvent was removed in vacuo. The crude product was purified by silica gel chromatography to yield 5.7 mg (21%) of **2** as an orange-red crystalline solid: ^{1}H NMR (CD_3CN) δ 0.950 [3H, t, J = 7.4 Hz, −NH(CH$_2$)$_3$C**H**$_3$], 1.220 (3H, t, J = 7.5 Hz, −CH$_2$C**H**$_3$), 1.412 [2H, m, −NH(CH$_2$)$_2$C**H**$_2$CH$_3$], 1.630 (2H, m, −NHCH$_2$C**H**$_2$CH$_2$CH$_3$), 2.460 (2H, dq, J = 1.0, 7.5 Hz, −C**H**$_2$CH$_3$), 3.240 (2H, m, J = 8.1 Hz, −NHC**H**$_2$CH$_2$CH$_2$CH$_3$), 5.231 (1H, br s, −NH), 5.940 (1H, s, 6-H), 7.240 (1H, s, 3-H), 7.267−7.656 (5H, m, −C$_6$H$_5$), 14.775 (1H, br s, −OH); ^{13}C NMR (CD_3CN) δ 13.4, 14.1, 20.9, 23.3, 31.5, 43.6, 96.9, 120.3, 123.9, 128.4, 130.3, 132.0, 132.4, 149.8, 153.4, 162.2; MS (EI) *m*/*z* 297 (M^+, 100%), 192 (M^+ − $C_6H_5N_2^+$, 50%); HRMS (EI) $C_{18}H_{23}N_3O$ (M^+) calcd 297.18411, obsd 297.18467.

(J) NMR Assignment of 2. ^{1}H and ^{13}C NMR spectra were obtained on a Bruker AM-500 spectrophotometer fitted with an inverse ^{1}H−^{13}C probe operating at a proton frequency of 500.14 MHz for protons. The spectra were recorded for a CD_3CN solution containing 11 mg (0.037 mmol) of **2** in a 5 mm NMR tube. ^{1}H chemical shifts were relative to residual CH_3CN set to 1.940 ppm. ^{13}C chemical shifts were relative to the ^{13}C signal of CD_3CN set to 118.2 ppm. The NOESY spectrum was acquired at a mixing time of 2 s at 27 °C. The details of the NMR assignment of **2** are available in the Supporting Information.

(K) Synthesis of a 4-Nitrophenylhydrazine Adduct of $\mathbf{1}_{ox}$ (10). A stirred solution of 4-nitrophenylhydrazine (316.8 mg, 2.1 mmol) in acetic acid (20 mL) was heated to 100 °C, and then $\mathbf{1}_{ox}$ (82.8 mg, 0.4 mmol) was added as an acetic acid solution. The reaction mixture was stirred at 100 °C for 1 h and cooled to room temperature. Water (50 mL) was added, and the mixture was neutralized by addition of $NaHCO_3$

and then extracted with diethyl ether. The combined organic layers were washed with water and dried with $MgSO_4$, and the solvent was removed in vacuo. The crude product was purified by silica gel chromatography to yield 38 mg (30%) of **10** as an orange-red crystalline solid: ^{1}H NMR ($CDCl_3$) δ 0.990 [3H, t, J = 7.3 Hz, $-NH(CH_2)_3C\mathbf{H}_3$], 1.298 (3H, t, J = 7.3 Hz, $-CH_2C\mathbf{H}_3$), 1.456 [2H, m, $-NH(CH_2)_2C\mathbf{H}_2CH_3$], 1.694 (2H, m, $-NHCH_2C\mathbf{H}_2CH_2CH_3$), 2.420 (2H, q, J = 7.3 Hz, $-C\mathbf{H}_2CH_3$), 3.263 (2H, m, $-NHC\mathbf{H}_2CH_2CH_2CH_3$), 4.849 (1H, br s, $-NH$), 5.788 (1H, s, ring proton at C_6), 6.951 (1H, s, ring proton at C_3), 7.573 (2H, d, J = 9.2 Hz), 8.245 (2H, d, J = 9.2 Hz), 16.132 (1H, br s, $-OH$); MS (EI) m/z 342 (M^+, 100%), 192 ($M^+ - C_6H_4N_3O_2^+$, 42%); HRMS (EI) $C_{18}H_{22}N_4O_3$ (M^+) calcd 342.16973, obsd 342.16920.

(L) Synthesis of a Phenylhydrazine Adduct of 4 (11). A stirred solution of phenylhydrazine hydrochloride (10.5 g, 72.5 mmol) in glacial acetic (20 mL) was heated to 100 °C, and then **4** (2.3 g, 14.5 mmol) was added as an acetic acid solution. The reaction mixture was stirred at 100 °C for 30 min and then cooled to room temperature. Hexanes (200 mL) were added, and the precipitated unreacted phenylhydrazine hydrochloride salt was removed by vacuum filtration. The precipitate was washed five times with 50 mL portions of hexanes. The combined hexane layer was washed three times with water and then dried over $MgSO_4$. Removal of the solvent in vacuo yielded a dark orange-brown solid, which was dissolved in a minimum volume of chloroform and applied to silica gel column chromatography. Elution with chloroform and ethyl acetate (4/1 v/v) and subsequent removal of the solvent gave **11** as dark red needles (350 mg, 10% yield): ^{1}H NMR ($CDCl_3$) δ 1.278 (3H, t, J = 7.6 Hz, $-CH_2C\mathbf{H}_3$), 2.628 (2H, q, J = 7.6 Hz, $-C\mathbf{H}_2CH_3$), 6.372 (1H, s, ring proton at C_3), 7.397 (1H, m), 7.484 (2H, m), 7.599 (1H, s, ring proton at C_6), 7.776 (2H, d), 13.868 (1H, s, $-OH$); ^{1}H NMR [$(CD_3)_2CO$] δ 1.204 (3H, t, J = 7.6 Hz), 2.664 (2H, q, J = 7.6 Hz), 6.783 (1H, s, ring proton at C_3), 7.368 (1H, s, ring proton at C_6), 7.442−7.543 (3H, m), 8.317 (1H, s, $-OH$), 11.848 (1H, s, $-OH$); ^{13}C NMR [$(CD_3)_2CO$] δ 13.2, 23.4, 114.6, 117.7, 122.0, 129.4, 130.8, 135.8, 139.0, 147.0, 148.3, 151.1.

(M) Deuterium Exchange of the Ring Proton of $\mathbf{1}_{ox}$, 4, and 8. NMR samples of quinones (4 mg) were prepared in D_2O (0.5 mL) and CD_3OD (0.5 mL). Spectra were taken at different time intervals. Changes in integration of the proton signal were used to monitor the deuterium exchange of the protons.

(N) Acid−Base Titration. The acid−base dissociation constants were determined in HCl for pH 0−1.0, $H_3PO_4 + KH_2PO_4$ for pH 1.5−3.0, $CH_3COOH + CH_3COOK$ for pH 3.0−6.0, $KH_2PO_4 + K_2HPO_4$ for pH 5.7−7.8, Tris for pH 8.0−8.8, $KHCO_3 + K_2CO_3$ for pH 9.0−11.0, K_2HPO_4 + KOH for pH 9.1−12.0, and KOH for pH 11.9−13.2. All buffer solutions had a concentration of 0.1 M, and their ionic strength was adjusted to 0.3 with KCl.

pK_as of $\mathbf{1}_{ox}$: The stock solution of $\mathbf{1}_{ox}$ was prepared by oxidation of the catechol ($\mathbf{1}_{red}$) in situ. $\mathbf{1}_{red}$·HCl (2.71 mg, 11.0 mmol) was dissolved in 1 mL of a 0.1 M potassium phosphate buffer (pH 6.7, I = 0.3 with KCl) and subjected to autoxidation in air, resulting in a quinone stock solution of $\mathbf{1}_{ox}$ (1.10×10^{-2} M). A 10 μL aliquot of the stock solution was then diluted with 990 μL of the appropriate buffer with the desired pH value. UV−vis spectra of the samples were taken immediately (7 s) after the dilution.

pK_as of $\mathbf{1}_{red}$: A stock solution of $\mathbf{1}_{red}$ prepared from $\mathbf{1}_{red}$·HCl (3.46 mg, 14.1 mmol) dissolved in 1 mL of 0.1 N HCl. A buffer solution (3 mL) in a quartz cell fused to an 8 cm graded seal tube, which was tightly closed with a septum rubber cap, was degassed by purging with O_2-free Ar gas for 15 min. O_2 was removed from the Ar gas by passage through an alkaline pyrogallol solution. An excess amount of $NaBH_4$ (23.5 molar equiv) was added to all buffers at pH >8. Twenty microliters of the stock solution of $\mathbf{1}_{red}$ was then added by a gastight syringe into the degassed buffer solution. The spectra were taken immediately after the dilution.

pK_as of $\mathbf{3}_{ox}$: $\mathbf{3}_{red}$·HCl (5.1 mg, 19.6 mmol) was dissolved in H_2O containing 1 mL of CH_3CN. The solution was neutralized by adding 1 μL of 50% NaOH and $\mathbf{3}_{red}$ subjected to autoxidation in air, resulting in a stock solution of $\mathbf{3}_{ox}$ (7.85×10^{-2} M, pH 6.46). A 100 μL aliquot of the stock solution was diluted with 900 μL of a buffer at the desired pH value. UV−vis spectra of the samples were taken immediately (7 s) following dilution.

pK_as of **8**, **2**, and **11**: A 40 μL aliquot of the appropriate CH_3CN stock solution ([**8**] = 2.4 mM, [**2**] = 0.46 mM, [**11**] = 0.37 mM) was diluted into 960 μL of an aqueous buffer at the desired pH. UV−vis spectra of the samples were taken immediately after the dilution.

(O) Electrochemistry. Cyclic voltammetry was carried out on a BAS 100A electrochemical analyzer at the desired pH with a three-electrode system consisting of a gold working electrode (electrode area = 0.02 cm^2), a coiled platinum counter electrode, and a saturated calomel electrode as the reference. The voltammetric measurements were performed with a potentiostat (Princeton Applied Research 173) in conjunction with a triangular wave generator (Princeton Applied Research 175) and recorded on a X-Y recorder (Kipp and Zonen). Prior to each experimental run, the gold working electrode was cleaned with a mixture of concentrated sulfuric acid and chromic acid, washed with purified, deionized distilled water, dried by N_2 flow, and transferred rapidly to the electrochemical cell containing the test solution. The experiments were carried out in Ar-purged solutions under an Ar atmosphere at room temperature. For the cyclic voltammetry of $\mathbf{3}_{ox}$, **8**, **9**, and $\mathbf{13}_{red}$, the buffer solution used in the assay was 0.1 M potassium phosphate (pH 6.74 ± 0.01) with I = 0.3 (KCl). For the pH titration of $\mathbf{1}_{ox}$, the buffers used were as described for the UV−vis assay. Sample solutions of quinones were prepared in 10 mL of the same potassium phosphate buffer at a final concentration of 10^{-3}−10^{-5} M. All sample solutions were freshly prepared and subjected to the measurement immediately.

(P) Reaction of 4-Ethylphenol or 4-Ethylcatechol with *N*-Methyl-*n*-butylamine in the Presence of Tyrosinase. A 10 μL aliquot of a stock solution of 4-ethylphenol or 4-ethylcatechol (20 mM in 2 mM HCl) and 0.1 mL of a stock solution of *N*-methyl-*n*-butylamine (0.2 M in 0.1 M potassium phosphate buffer, pH 7.2) were added to a quartz cuvette containing 0.876 mL of a 0.1 M potassium phosphate buffer (pH 7.2) which had been preequilibrated at 25 ± 0.2 °C. A 14 μL aliquot of a mushroom tyrosinase stock solution (14 μg/mL) was then added to the cuvette. The spectra of the reaction mixture were periodically recorded with a HP photodiode array spectrophotometer.

(Q) Reaction of 4-Ethylcatechol and *N*-Methyl-*n*-butylamine in the Presence of $NaIO_4$. A 10 μL aliquot of a stock solution of 4-ethylcatechol (20 mM in 2 mM HCl) and a 10 μL aliquot of the stock solution of *N*-methyl-*n*-butylamine (0.2 M in 0.1 M potassium phosphate buffer, pH 7.2) were added to a quartz cuvette containing 0.97 mL of 0.1 M potassium buffer (pH 7.2) that had been preequilibrated at 25 ± 0.2 °C. A 10 μL aliquot of a $NaIO_4$ stock solution (0.2 M in 0.1 M potassium phosphate buffer, pH 7.2) was then added to the cuvette. The spectra of the reaction mixture were periodically recorded with a HP photodiode array spectrophotometer.

Results and Discussion

Synthesis and Characterization of LTQ Model Compounds. (A) Synthesis of $\mathbf{1}_{ox}$. 4-*n*-Butylamino-5-ethyl-1,2-benzoquinone ($\mathbf{1}_{ox}$) is a simplified analogue of the LTQ cofactor having the same functional groups but lacking a peptidyl backbone. Initially, we attempted to isolate $\mathbf{1}_{ox}$ from the reaction of *n*-butylamine with 4-ethyl-1,2-benzoquinone. This strategy proved unsuccessful as the chemistry is not clean, and a number of side products formed in the reaction mixture. Ultimately, $\mathbf{1}_{ox}$ was prepared from 6-nitropiperonal via a five-step synthesis, as shown in Scheme 1. The stability of $\mathbf{1}_{ox}$ varies depending on the conditions under which it is prepared. Decomposition of $\mathbf{1}_{ox}$ was observed when concentrated in organic solvents (precipitates as dark brown mass). We found that $\mathbf{1}_{ox}$ can be

Scheme 1. Synthesis of $\mathbf{1}_{ox}$

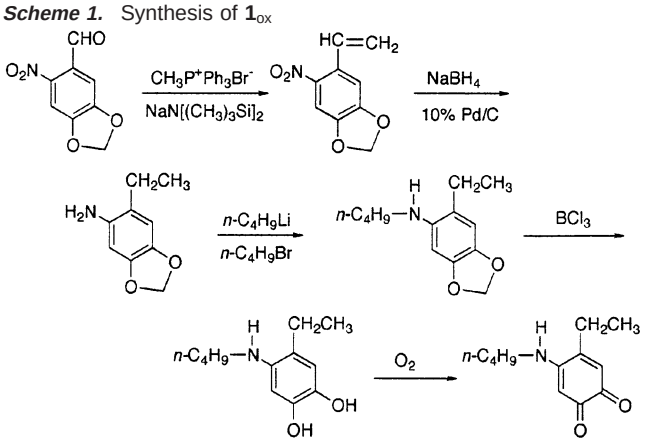

isolated by lyophilization of an aqueous solution at neutral pH following air oxidation of the catechol ($\mathbf{1}_{red}$).

The ^{1}H NMR of $\mathbf{1}_{ox}$ showed two proton resonances at 5.140 and 6.154 ppm, corresponding to the quinonoid ring protons. The resonance at 6.154 ppm showed a long-range coupling to the methylene proton of the ethyl side chain at C_5 and thus was assigned to H_6 (J = 1.5 Hz). The same coupling was seen for H_6 of **4**, a TPQ model compound with an ethyl side chain at C_5. The resonance at 5.140 ppm was consequently assigned as H_3. The two ring protons of an *o*-quinone with a methoxy side chain (**7**) had been previously assigned as H_3 at 5.760 ppm and H_6 at 6.200 ppm, respectively.[37] The H_3 of $\mathbf{1}_{ox}$ is 0.62 ppm upfield shifted compared to that of **7**, reflecting the electron-donating nature of the nitrogen lone pair of the *n*-butylamino side chain. It should be noted that the ring protons of an anionic TPQ model compound (**4**) have chemical shifts very close to those of $\mathbf{1}_{ox}$. However, in contrast to **4**, no deuterium exchange of H_3 was observed for $\mathbf{1}_{ox}$ (see below).

(B) UV−Vis Spectra of Model Compounds. Perhaps the most accessible feature of quinoproteins is their prominent visible absorption spectra. However, these spectra can often be misleading when attempting to assign the nature of the quinonoid cofactor. The UV−vis spectra of LTQ model compounds $\mathbf{1}_{ox}$ and $\mathbf{3}_{ox}$ are shown in Figure 1 together with those of TPQ model compounds (**4**, **5**) and *p*-quinones bearing an *n*-butylamino side chain (**8**, **9**). The spectrum of $\mathbf{1}_{ox}$ displays an absorption band with a λ_{max} at 298 nm and a broad absorption band with a λ_{max} around 504 nm, which is an excellent match to that of LTQ in LOX.[27,48] The ratio of the absorbances at 298 and 504 nm (A_{298}/A_{504}) of $\mathbf{1}_{ox}$ is 3.9. Both λ_{max} of $\mathbf{1}_{ox}$ are ca. 20 nm red shifted compared to those of **4**. At pH 7.0, the visible spectrum of $\mathbf{1}_{ox}$ is close to that of **4**, so this alone cannot be relied upon for cofactor identification (Figure 1a).

In contrast to TPQ, no spectral changes were observed for $\mathbf{1}_{ox}$ over the physiological pH range (4−8). Methylation of the nitrogen of $\mathbf{1}_{ox}$ ($\mathbf{3}_{ox}$) resulted in a 20 nm red shift of both absorption maxima, and the ratio of A_{316}/A_{528} was reduced to 2.6 (Figure 1b). A similar red shift was observed upon N-methylation (**9**) of a *p*-quinone with an *n*-butylamino side chain (**8**) (Figure 1c). These results suggest that $\mathbf{1}_{ox}$ exists as a neutral *o*-quinone in which the NH proton is retained on the *n*-butylamino side chain. At pH 7, **4** exists as a monoanion where the C_2 hydroxyl group is deprotonated.[36,38] The red color of **4** results from the delocalization of this negative charge into the quinone ring (eq 1).

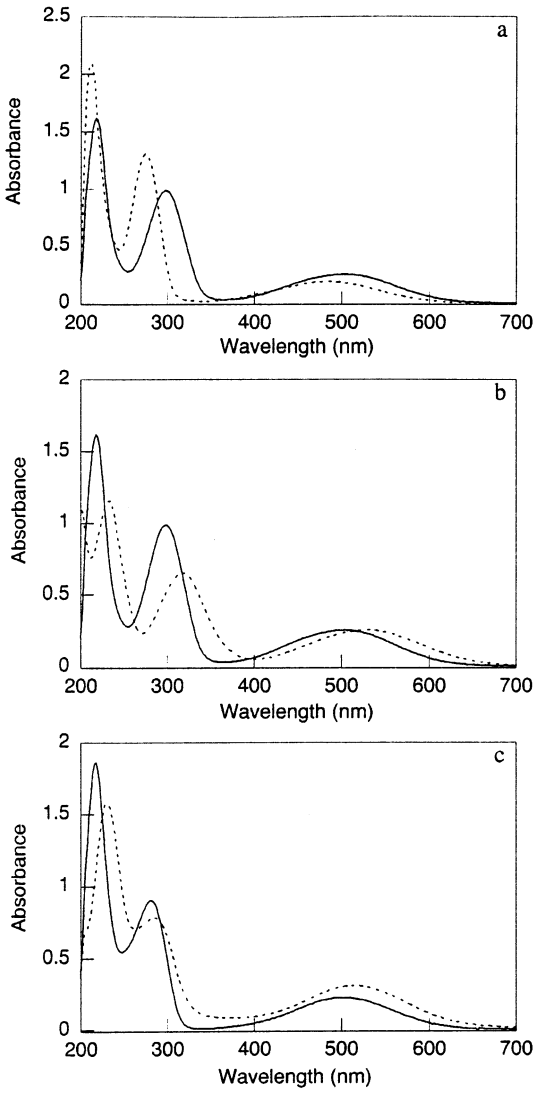

Figure 1. (a) UV−vis spectra of $\mathbf{1}_{ox}$ (—) and **4** (- - -). (b) UV−vis spectra of $\mathbf{1}_{ox}$ (—) and $\mathbf{3}_{ox}$ (- - -). (c) UV−vis spectra of **8** (—) and **9** (- - -). All spectra are for 0.1 mM of the appropriate model compound in 0.1 M potassium phosphate (pH = 7.0, I = 0.3 with KCl).

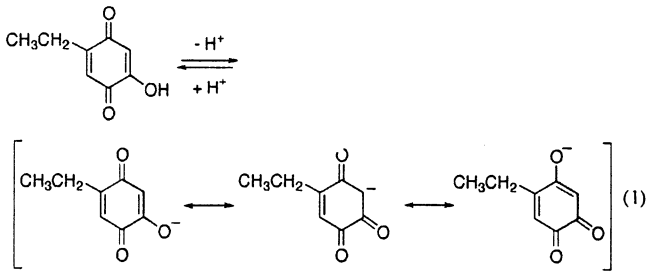

The delocalization was confirmed for **4** and TPQ in CAO by resonance Raman spectroscopy where the C_3 ring proton was shown to exchange with solvent water.[52] In the model chemistry, NMR was also used to confirm that H_3 of **4** could exchange with solvent.[36,37] As the UV−vis spectra of $\mathbf{1}_{ox}$ and $\mathbf{3}_{ox}$ are close to that of **4**, one might presume that LTQ has similar electronic properties to TPQ. We looked for deuterium exchange of the quinonoid ring protons on $\mathbf{1}_{ox}$, **4**, and **8** in D_2O and CD_3OD by ^{1}H NMR spectroscopy. For $\mathbf{1}_{ox}$, only the NH proton of the

(52) Moenneloccoz, P.; Nakamura, N.; Steinebach, V.; Duine, J. A.; Mure, M.; Klinman, J. P.; Sandersloehr, J. *Biochemistry* **1995**, *34*, 7020−7026.

n-butylamino side chain showed exchange with deuterium, and no incorporation of deuterium on the quinonoid ring was detected even after 7 days of incubation. The same exchange pattern was observed for **8**. In contrast, the proton at C-3 (H_3) of **4** disappeared rapidly (within the minimal acquisition time $<2-3$ min) in D_2O. In CD_3OD, the exchange was much slower, taking hours to complete. This is because **4** exists predominantly as the neutral *p*-quinone form in methanol.

These observations are consistent with resonance Raman spectroscopic studies of LTQ in LOX, which showed that the quinonoid ring proton was not exchangeable with D_2O.[48] The absence of exchange at pH 7 implies that LTQ and $\mathbf{1}_{ox}$ exist as only the *o*-quinone under these conditions, i.e., that there are no resonance forms which provide a pathway for the exchange of the ring protons.

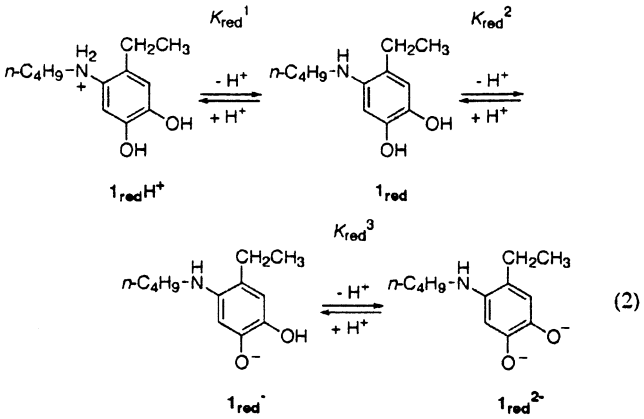

(2)

(C) Acid−Base Properties of $\mathbf{1}_{red}$. The pK_a values for $\mathbf{1}_{red}$ (pK_{red}^1, pK_{red}^2, pK_{red}^3 in eq 2) were determined spectrophotometrically under anaerobic conditions. In acidic solution, O_2 is removed from the buffer by purging with Ar gas prior to the addition of the hydrochloride salt of $\mathbf{1}_{red}$. Above pH 8, it was necessary to add an excess of $NaBH_4$, in addition to removing O_2, to reverse the oxidation of $\mathbf{1}_{red}$ as this reaction becomes very rapid at alkaline pH. At pH <4, $\mathbf{1}_{red}$ shows a λ_{max} at 282 nm which red shifts with increasing pH (300 nm at pH 7, 310 nm at pH 13) as shown in Figure 2a. Two pK_as, calculated to be 5.97 ± 0.05 and 9.39 ± 0.07, respectively, were obtained by least-squares fitting of the absorbance change at 310 nm (Figure 2b). The former pK_a is assigned to the deprotonation of the amino group of the *n*-butylamino side chain (pK_{red}^1), and the latter is assigned to one of the hydroxyl groups (pK_{red}^2), presumably at C_2. The pK_a of the remaining hydroxyl group (pK_{red}^3) is estimated to be greater than 13 but could not be accurately determined by the UV−vis spectroscopic pH titration (see Electrochemistry). The value of pK_{red}^1 is very close to that of the amino group of the aminoresorcinol form of TPQ (5.88).[36] The protonation of this amino group yielded spectroscopic changes similar to those observed for $\mathbf{1}_{red}$, i.e., a blue shift in λ_{max} resulting in no absorbance above 300 nm. This analogy was used, in part, for the assignment of pK_{red}^1. At neutral pH, $\mathbf{1}_{red}$ has a λ_{max} at 300 nm which is 10 nm blue shifted when compared to the aminoresorcinol form of TPQ. Further, $\mathbf{1}_{red}$ lacks the secondary features below 280 nm, which are observed for the aminoresorcinol form of TPQ at pH 7−9. pK_{red}^2 was assigned to the C_2 hydroxyl group because the C_1 hydroxyl group has a decreased pK_a as a result of it being para to the electron-donating *n*-butylamino side chain at C_4. Once deprotonation has occurred, it is possible that the proton on the monoanion form of $\mathbf{1}_{red}$ is equally shared between the oxygens at C_1 and C_2.

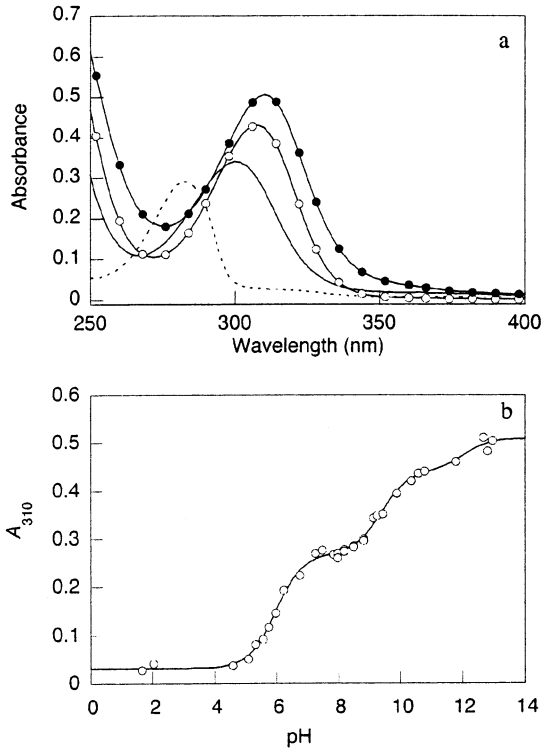

Figure 2. (a) Absorption spectra of $\mathbf{1}_{red}$ at pH 1.65 (- - -), $\mathbf{1}_{red}$ at pH 7.25 (—), $\mathbf{1}_{red}$ at pH 10.36 (○), and $\mathbf{1}_{red}$ at pH 12.97 (●), where $[\mathbf{1}_{red}] = 9.3 \times 10^5$ M. (b) Spectroscopic pK_a determination for $\mathbf{1}_{red}$. The line was drawn by a least-squares fit using the equation $A_{310} = \{(\epsilon_{310}{}^{\mathbf{1}_{red}H^+}[H^+]^3 + \epsilon_{310}{}^{\mathbf{1}_{red}} K_{red}^1[H^+]^2 + \epsilon_{310}{}^{\mathbf{1}_{red}^-} K_{red}^1 K_{red}^2[H^+] + \epsilon_{310}{}^{\mathbf{1}_{red}^{2-}} K_{red}^1 K_{red}^2 K_{red}^3)/([H^+]^3 + K_{red}^1[H^+]^2 + K_{red}^1 K_{red}^2[H^+] + K_{red}^1 K_{red}^2 K_{red}^3)\}[\mathbf{1}_{red}]_T$.

(D) Acid−Base Properties of $\mathbf{1}_{ox}$ and $\mathbf{3}_{ox}$. A decrease in pH from 4 to 1 resulted in a bleaching of the characteristic broad absorption band of $\mathbf{1}_{ox}$ at 504 nm (Figure 3a). A plot of A_{504} vs pH was fit to the titration curves for the dissociation of a single proton, allowing the calculation of a pK_a of 1.65 ± 0.04 (Figure 3b). This corresponds to that of the amino side chain of $\mathbf{1}_{ox}$ (pK_{ox}^1 in eq 3). $\mathbf{3}_{ox}$ showed a similar spectral change upon acidification and gave an acidic pK_a value very close to that of $\mathbf{1}_{ox}$ (p$K_a = 1.96 \pm 0.03$) (data not shown).

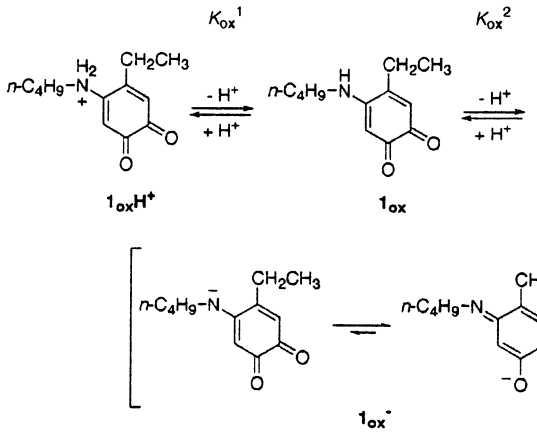

(3)

It was difficult to determine whether $\mathbf{1}_{ox}$ has any pK_a at alkaline pHs (above 9) due to the instability of this species under

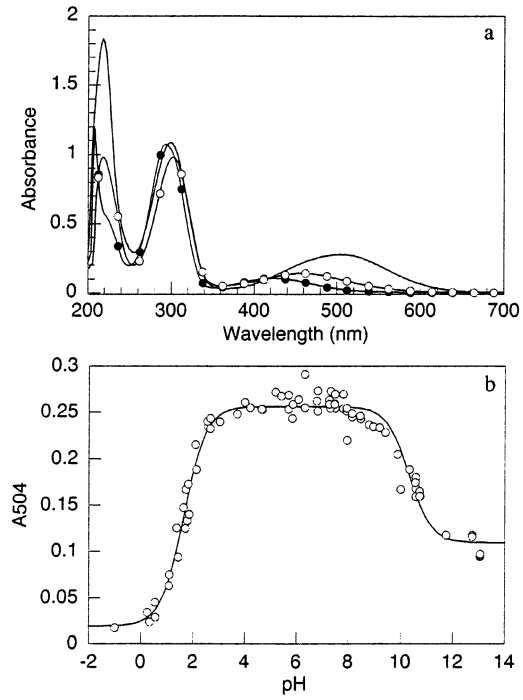

Figure 3. (a) Absorption spectra of (●) $\mathbf{1}_{ox}$ at pH 0.34, (—) $\mathbf{1}_{ox}$ at pH 7.32, and (○) $\mathbf{1}_{ox}$ at pH 11.75. $[\mathbf{1}_{ox}] = 1.1 \times 10^{-4}$ M. (b) Spectroscopic pK_a determination for $\mathbf{1}_{ox}$. The line was drawn by a least-squares fit using the equation $A_{504} = \{(\epsilon_{504}{}^{\mathbf{1}_{ox}H^+}[H^+]^2 + \epsilon_{504}{}^{\mathbf{1}_{ox}}K_{ox}{}^1[H^+] + \epsilon_{504}{}^{\mathbf{1}_{ox}^-}K_{ox}{}^1K_{ox}{}^2)/([H^+]^2 + K_{ox}{}^1[H^+] + K_{ox}{}^1K_{ox}{}^2)\}[\mathbf{1}_{ox}]_T$.

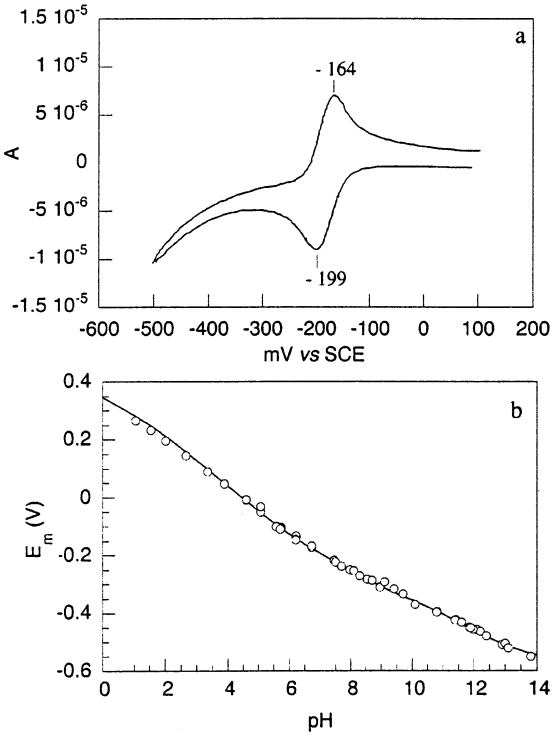

Figure 4. (a) Cyclic voltammogram of $\mathbf{1}_{ox}$ at pH 6.7 at a scan speed of 100 mV s^{-1}. $[\mathbf{1}_{ox}] = 9.8 \times 10^{-5}$ M. The direction of the scan is from positive to negative. (b) E_m—pH diagram for $\mathbf{1}_{ox}$. The line was drawn by a least-squares fit using the equation $E_m = E_0 + (RT/2F)\log\{([H^+]^4 + K_{red}{}^1[H^+]^3 + K_{red}{}^1K_{red}{}^2[H^+]^2 + K_{red}{}^1K_{red}{}^2K_{red}{}^3[H^+])/([H^+]^2 + K_{ox}{}^1[H^+] + K_{ox}{}^1K_{ox}{}^2)\}$.

basic conditions. The UV—vis spectra of $\mathbf{1}_{ox}$ were acquired within 7 s from mixing of the stock solution with the appropriate buffer. Upon increasing pH, a blue shift of the λ_{max} from 504 to 460 nm was observed (Figure 3a). A pK_a of 10.33 ± 0.07 was calculated from the absorbance changes at 504 nm, possibly corresponding to the proton of the *n*-butylamino side chain (Figure 3b). However, there was an interfering but distinct absorbance change from bleaching of the characteristic visible absorbances observed concomitant with an increase in absorbance at 282 nm and isosbestic points at 290 and 250 nm (data not shown). This latter change was irreversible and also accelerated with increasing pH ($t_{1/2}$ = 500 s at pH 10.8). As this occurs outside of the physiological pH range, we did not pursue the characterization of the reaction product in this study. $\mathbf{3}_{ox}$ has no pK_a above 10 but was also unstable, undergoing time-dependent spectral changes similar to those observed for $\mathbf{1}_{ox}$.

(E) Electrochemistry. The cyclic voltammogram of $\mathbf{1}_{ox}$ at pH 6.7 (Figure 4a) reveals a single process for the oxidation and reduction to give a midpoint potential of $\mathbf{1}_{ox}$ of −0.182 V (vs SCE). The peak separation of the anodic and cathodic peaks (ΔE_p) is 35 mV, which is very close to the theoretical value for a reversible concerted two-electron reaction (30 mV).

In Table 1, the midpoint potentials of model compounds at pH 6.7 are summarized. $\mathbf{1}_{ox}$ and **4** have very similar redox potentials as might be expected since the cofactors that they model catalyze similar reactions (i.e., primary amine oxidation). Although **8** shows a UV—vis absorbance spectrum similar to those of $\mathbf{1}_{ox}$ and **4**, its E_m is ca. −0.1 V negative when compared to $\mathbf{1}_{ox}$ and **4**. N-Methylation of the *n*-butylamino side chain of $\mathbf{1}_{ox}$ resulted in a large positive shift of E_m (+0.145 V), yielding a value for $\mathbf{3}_{ox}$ very close to that of **7**. A positive shift of E_m was also observed for **9** vs **8**, but the ΔE_m was small (0.041 V). These results suggest that methylation of the *n*-butyl side chain of $\mathbf{1}_{ox}$ has a significant effect on the electronic nature of the quinonoid ring, as discussed in the context of its ^{1}H NMR properties.

Table 1. Midpoint Potentials of Model Compounds at pH 6.7

model compd	E_m (V) vs SCE	model compd	E_m (V) vs SCE
$\mathbf{1}_{ox}$	−0.182[a]	**7**	−0.032[b]
$\mathbf{3}_{ox}$	−0.037	**8**	−0.331
4	−0.181	**9**	−0.290
6	+0.109[b]	$\mathbf{13}_{ox}$	−0.108

[a] Reference 27. [b] Reference 37.

Electrochemical redox potentials of $\mathbf{1}_{ox}$ were measured as a function of pH. Between pH 1.10 and pH 13.95, cyclic voltammograms showing a single process for the reduction and oxidation of $\mathbf{1}_{ox}$ were obtained. Between pH 1 and pH 3, ΔE_p was 30 mV, which is in agreement with the theoretical value for a reversible concerted two-electron reaction. With increasing pH, the ΔE_p value increased (maximum of 45 mV) to give a quasi-reversible cyclic voltammogram. No decomposition of $\mathbf{1}_{ox}$ was observed within the time scale of the CV scans.

Figure 4b is a plot showing the pH dependence of the midpoint potentials of the overall $2e^-$ $\mathbf{1}_{ox}/\mathbf{1}_{red}$ couple. The solid line was generated using the values of pK_as of $\mathbf{1}_{ox}$ (p$K_{ox}{}^1$ and p$K_{ox}{}^2$) and $\mathbf{1}_{red}$ (p$K_{red}{}^1$ and p$K_{red}{}^2$) calculated from the UV—vis spectroscopic titrations (see Figures 3b and 2b). The third pK_a of $\mathbf{1}_{red}$ (p$K_{red}{}^3$) was then calculated to be 12.96 ± 0.19 from the least-squares curve fitting. When the fitting was performed with p$K_{ox}{}^2$ and p$K_{red}{}^3$ as variables (fit not shown), they were calculated as 10.52 ± 0.09 and 13.42 ± 0.35, respectively. The value of p$K_{ox}{}^2$ matches very well with that obtained from UV—

vis spectroscopic pH titration (Figure 3b). Further, a good fit of the data could not be obtained without including pK_{ox}^2, suggesting that this pK_a is not an artifact of the irreversible time-dependent bleaching seen in the UV−vis spectra at high pH.

The fit of the E_m vs pH plot (Figure 4b) is consistent with five linear regions with slopes of −60 mV/pH (pH 1−1.6), −90 mV/pH (pH 2−5.8), −60 mV/pH (pH 6−9.3), −30 (pH 9.6−10.8), and −60 mV/pH (pH 11.4−13.3), respectively. Scheme 2 shows a summary of the species involved in the E_m−pH diagram of $\mathbf{1}_{ox}$. Below pH 2, the protonated $\mathbf{1}_{red}$ is oxidized to the protonated quinone in a $2H^+$, $2e^-$ process to give a slope of −60 mV/pH. Between pH 2 and pH 5.8, the slope of −90 mV/pH corresponds to a $3H^+$, $2e^-$ redox process due to the acid dissociation of the *n*-butylamino side chain of $\mathbf{1}_{ox}$ (pK_{ox}^1). Between pH 6 and pH 9.3, the *n*-butylamino side chain of $\mathbf{1}_{red}$ is deprotonated ($pK_{red}^1 = 5.97$) and undergoes a $2H^+$, $2e^-$ oxidation to $\mathbf{1}_{ox}$, resulting in a slope of −60 mV/pH. Between pH 9.6 and pH 10.8, the second acid dissociation of $\mathbf{1}_{red}$ ($pK_{red}^2 = 9.39$) gives a slope of 30 mV/pH, corresponding to a $1H^+$, $2e^-$ process. Between pH 11.4 and pH 13.3, the second acid dissociation of $\mathbf{1}_{ox}$ ($pK_{ox}^2 = 10.33$) gives a slope of 60 mV/pH, corresponding to a $2H^+$, $2e^-$ process. Above pH 13.3, the quinol is fully deprotonated ($pK_{red}^3 = 13.4$) to give a slope of 30 mV/pH, corresponding to a $1H^+$, $2e^-$ process.

Between pH 8.0 and pH 8.5, LOX shows maximum activity in the oxidation of *n*-hexylamine.[53] Under these conditions, from this study it can be seen that LTQ will most likely undergo the $2H^+$, $2e^-$ redox process of $\mathbf{1}_{ox}/\mathbf{1}_{red}$ (Scheme 2). The E_m value for the substrate-reduced form of TPQ, aminoresorcinol/iminoquinone couple, was determined to be −0.133 V vs SCE at pH 6.7, which is only slightly positive compared to that for TPQ_{ox}/TPQ_{red} (see Table 1).[36] The similarity in E_m values between $\mathbf{1}_{ox}$ and **4** suggests that their substrate-reduced forms may be similar in their reactivities toward O_2.

Synthesis and Characterization of the Phenylhydrazine (2) and 4-Nitrophenylhydrazine Adducts (10) of $\mathbf{1}_{ox}$. The identification of LTQ in LOX was achieved by following the same experimental procedures used for identifying TPQ in CAOs.[26,27] LOX was inhibited with phenylhydrazine to covalently modify LTQ to form a stable phenylhydrazine adduct. The modified LTQ-containing peptide was isolated and then characterized by Edman degradation, mass spectrometry, and resonance Raman spectroscopy. To identify the structure of derivatized LTQ, a model compound (**2**) mimicking the proposed cofactor structure was synthesized. Resonance Raman spectra of **2** were identical to that of the modified cofactor-containing peptide, confirming the presence of LTQ in LOX.[27] The position of the nucleophilic addition to LTQ has been proposed to be at C_1. We confirmed that **2** results from the addition of the hydrazine to the C_1 oxygen using a combination of HMQC, HMBC, and NOESY experiments. The details of these analyses are provided in the Supporting Information. **2** can undergo hydrazone−azo tautomerization (eq 4), and the NMR results suggest that the azo form is predominant in the equilibrium for **2**. This is similar behavior to that observed for **11** and **12**, the phenyl and 4-nitrophenylhydrazine adducts of the TPQ model compound, **4**.[36]

Scheme 2. Intermediates Deduced from E_m−pH Studies[a]

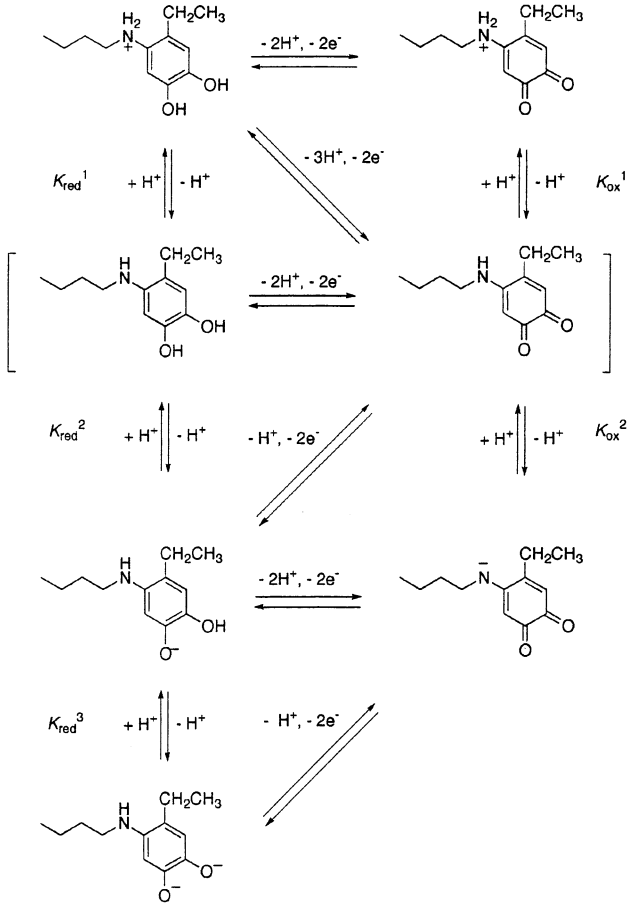

[a] The species in brackets are attributed to those on LOX between pH 8.0 and pH 8.5, conditions of maximal LOX activity.

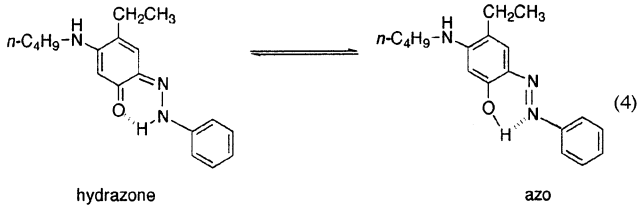

The UV−vis spectra of **2** and **11** at different pHs are shown in Figures 5a and 6a, respectively. At neutral pH, **2** shows λ_{max} at 446 nm that is red shifted (16 nm) vs **11**. At high alkaline pH (>13), both exhibit very similar absorbance properties with λ_{max} at 486 nm. The pK_a values for these spectral changes were calculated to be 11.90 ± 0.04 for **2** (from the absorbance changes at 446 and 486 nm shown in Figure 5c) and 12.83 ± 0.17 for **11** (from the absorbance changes at 430 and 486 nm shown in Figure 6d). These are assigned as the acid dissociation of the hydroxyl group at C-2 of **2** and **11** respectively, where both participate in a hydrogen-bonding interaction with an adjacent azo group (eqs 5 and 6).

As discussed below, at neutral pH, **11** exists as a monoanion in contrast to **2**, which is a neutral species; deprotonation from the monoanion of **11** makes the dissociation of second hydroxyl group harder. In this way, the 2-hydroxyl group of **2** has a pK_a value about 1 pH unit lower than that of the 4-hydroxyl group of **11**.

2 does not show a significant spectral change between pH 3.11 and pH 7, and the λ_{max} remains at 446 nm. In contrast, a

(53) Gacheru, S. N.; Trackman, P. C.; Kagan, H. M. *J. Biol. Chem.* **1988**, *263*, 16704−16708.

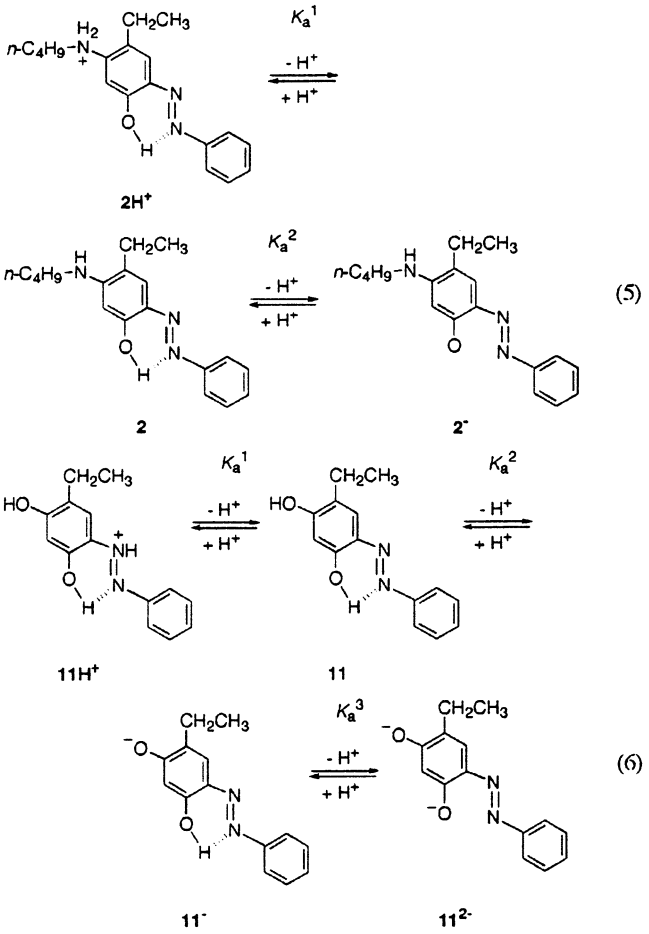

large spectral change was observed for **11** in this pH range. At pH 4.38, **11** shows a broad absorption band with λ_{max} at 388 nm. This shifts to 430 nm, with an isosbestic point, upon increasing the pH, giving a pK_a value of 5.93 ± 0.03 (Figure 6b). This indicates that **2** exists as a neutral species but **11** exists as a monoanion at physiological pH. **2** shows a large spectral change associated with the pK_a (2.12; Figure 5b) of the *n*-butylamino side chain, namely, a large red shift of the λ_{max} at 446 nm to 478 nm. Although **11** does exhibit a red shift of the λ_{max} at 388 nm to 430 nm by protonation of the hydrazone−azo group, it takes place below pH 2 (pK_a = −0.28; Figure 6a,d).

The pH-dependent spectral shifts of **11** at alkaline pH have been used to assign the presence of TPQ as a cofactor in CAOs.[54] In these experiments, the spectra of the hydrazone-inhibited (either phenyl or 4-nitrophenyl) enzyme at pH 7 were compared to those in 2 M KOH, and a shift in λ_{max} from ~442 to ~482 nm was taken as a positive identifier of TPQ. However, as a similar pattern was seen for both **2** and **11** under these conditions, this test alone cannot distinguish between the TPQ and LTQ cofactors in enzymes. We suggest that, in addition to using the basic pH shift, the spectra of the modified cofactors should also be monitored under acidic conditions. By analogy to the model systems, derivatized LTQ should show a red shift in the λ_{max} from 446 to 478 nm between pH 3 and pH 1, giving a spectrum distinct from that of derivatized TPQ (λ_{max} = 388 nm). Further reducing the pH below 1 should shift the λ_{max} of derivatized TPQ to 470 nm while leaving that of derivatized LTQ unchanged.

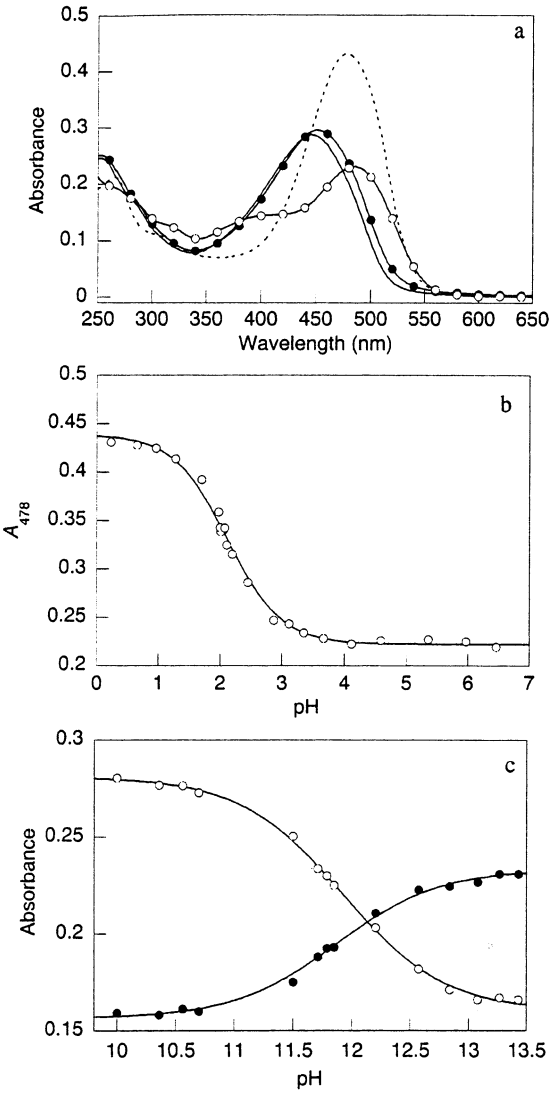

Figure 5. (a) Absorption spectra of (- - -) **2** at pH 0.23, (●) **2** at pH 3.11, (—) **2** at pH 7.01, and (○) **2** at pH 13.43. [**2**] = 2.3 × 10^{-5} M. (b) Spectroscopic determination of acidic pK_a for **2**. The line was drawn by a least-squares fit using the equation $A_{478} = \{(\epsilon_{478}{}^{2H^+}[H^+] + \epsilon_{478}{}^{2} K_a{}^{1})/([H^+] + K_a{}^{1})\}[\mathbf{2}]_T$. (c) Spectroscopic determination of basic pK_a for **2**: (●) absorbance at 486 nm and (○) absorbance at 446 nm. The line was drawn by a least-squares fit using the equations $A_{486} = \{(\epsilon_{486}{}^{2}[H^+] + \epsilon_{486}{}^{2^-} K_a{}^{2})/([H^+] + K_a{}^{2})\}[\mathbf{2}]_T$ and $A_{446} = \{(\epsilon_{446}{}^{2}[H^+] + \epsilon_{446}{}^{2^-} K_a{}^{2})/([H^+] + K_a{}^{2})\}[\mathbf{2}]_T$.

4-Nitrophenylhydrazine is generally used in preference to phenylhydrazine in detection of TPQ in CAOs, as the adduct resulting from the former has stronger UV−vis spectral features than that from the latter.[54] In contrast to **12**, **10** was found to be unstable in aqueous solution, and it was not possible to accurately determine the pK_a values of **10**, where an approximate value of 11.7 was measured (vs 12.2 for **12**[54]). In aqueous solution, **10** has a λ_{max} at 480 nm at 10 s after dilution from the CH_3CN stock solution, but time-dependent changes of the spectrum were observed at pH <9 (λ_{max} at 480 nm decreased and a new absorption built in at 600 nm). **10** did not show this spectral change in organic solvents and gave a λ_{max} of approximately 460 nm. Above pH 12, **10** was stable in aqueous solution and showed a λ_{max} at 572 nm, showing the similar base-

(54) Janes, S. M.; Palcic, M. M.; Scaman, C. H.; Smith, A. J.; Brown, D. E.; Dooley, D. M.; Mure, M.; Klinman, J. P. *Biochemistry* **1992**, *31*, 12147−12154.

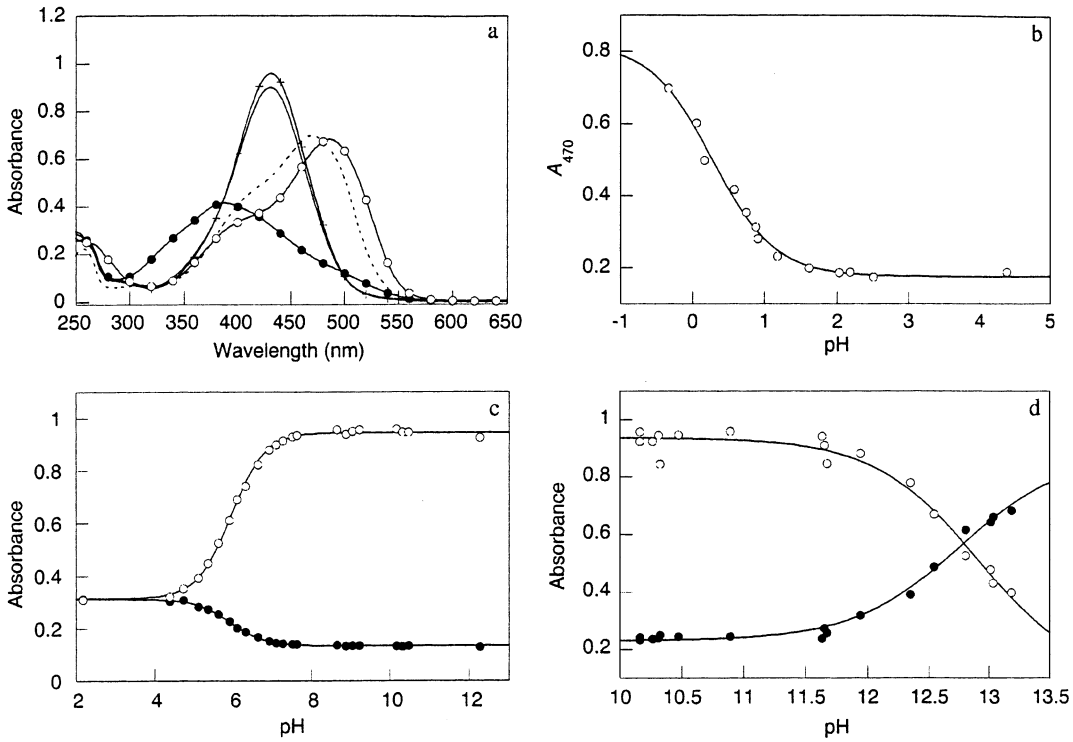

Figure 6. (a) Absorption spectra of (- - -) **11** at pH −0.33, (●) **11** at pH 4.38, (—) **11** at pH 7.10, (×) **11** at pH 10.16, and (○) **11** at pH 13.18. [**11**] = 1.9×10^{-5} M. (b) Spectroscopic determination of acidic pK_a (pK_a^1) for **11**. The line was drawn by a least-squares fit using the equation $A_{470} = \{(\epsilon_{470}^{\mathbf{11}H^+}[H^+] + \epsilon_{470}^{\mathbf{11}}K_a^1)/([H^+] + K_a^1)\}[\mathbf{11}]_T$. (c) Spectroscopic determination of the second pK_a (pK_a^2) for **11**: (●) absorbance at 350 nm and (○) absorbance at 430 nm. The line was drawn by a least-squares fit using the equations $A_{350} = \{(\epsilon_{350}^{\mathbf{11}}[H^+] + \epsilon_{350}^{\mathbf{11}^-}K_a^2)/([H^+] + K_a^2)\}[\mathbf{11}]_T$ and $A_{430} = \{(\epsilon_{430}^{\mathbf{11}}[H^+] + \epsilon_{430}^{\mathbf{11}^-}K_a^2)/([H^+] + K_a^2)\}[\mathbf{11}]_T$. (d) Spectroscopic determination of basic pK_a (pK_a^3) for **11**: (●) absorbance at 486 nm and (○) absorbance at 430 nm. The line was drawn by a least-squares fit using the equations $A_{486} = \{(\epsilon_{486}^{\mathbf{11}^-}[H^+] + \epsilon_{486}^{\mathbf{11}^{2-}}K_a^3)/([H^+] + K_a^3)\}[\mathbf{11}]_T$ and $A_{430} = \{(\epsilon_{430}^{\mathbf{11}^-}[H^+] + \epsilon_{430}^{\mathbf{11}^{2-}}K_a^3)/([H^+] + K_a^3)\}[\mathbf{11}]_T$.

Scheme 3. Proposed Pathway for Biogenesis of LTQ[a]

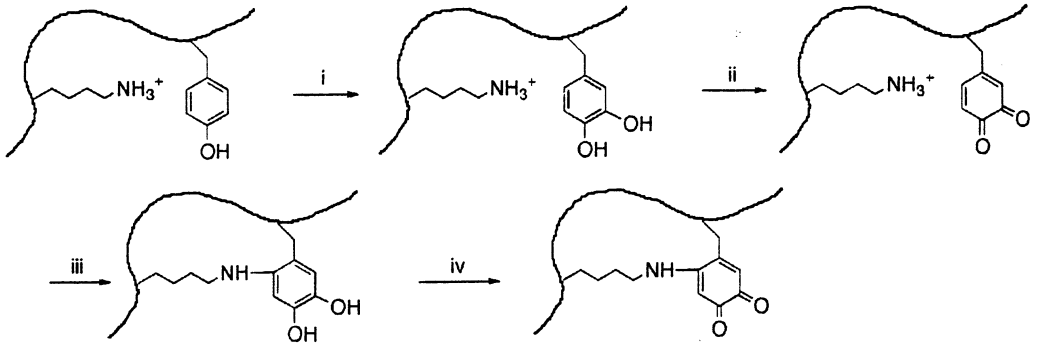

[a] Steps: (i) autocatalytic oxidation with O_2 and Cu^{2+} or exogenous enzyme catalysis; (ii) O_2 oxidation or exogenous enzyme catalysis; (iii) 1,4-addition; (iv) O_2 oxidation.

induced purple shift associated with the 4-nitrophenylhydrazine adduct of **4** (**12**).[54] Because of the unassigned spectral changes of **10** at neutral pH, derivatization with phenylhydrazine is recommended for identification and quantification of the LTQ cofactor in enzyme systems.

Model Study on Biogenesis of LTQ. The biogenesis of TPQ has been extensively studied. It is well accepted that TPQ is formed from a tyrosine residue at the active site via an autocatalytic mechanism, requiring Cu(II) at the active site and O_2, but no other enzymes.[32,35,55] At this juncture there is little known about the mechanism of the biogenesis of LTQ, mainly due to the absence of an expression system yielding an active enzyme in suitable quantities for detailed spectroscopic studies. We have proposed a mechanism based upon that of TPQ biogenesis,[27] in which the hydroxylation of a tyrosine residue at the active site, either autocatalytic or enzymatic, is followed by formation of dopaquinone, subsequent nucleophilic addition of ϵ-amino group of a lysine side chain, and air oxidation to yield LTQ (Scheme 3).

One of the intriguing aspects of LTQ biogenesis concerns the directionality of nucleophilic attack by a lysine side chain on the dopaquinone intermediate. In theory, lysine could add to dopaquinone via either a 1,2-, 1,4-, or 1,6-pathway. Naturally occurring *o*-quinones undergo nucleophilic addition by amino acids such as lysine, cysteine, and histidine, and this addition initiates polymerization. This process is known as quinone

(55) Schwartz, B.; Olgin, A. K.; Klinman, J. P. *Biochemistry* **2001**, *40*, 2954−2963.

tanning and is a source of pigmentation in plants, insects, and animals and also glue and varnish formation in mollusks.[56,57] Insect cuticles contain quinones that are cross-linked with histidine side chains and are the cause of sclerotization of the exoskeleton.[45,58] Cross-links between glutathione and *o*-quinone have been detected in flesh fly (*Sarcophaga peregrina*) infected with *Escherichia coli*, where this product is proposed to be involved in a self-defense mechanism against bacterial infection.[43,59] Studies of the reactions seen in insects have shown that the quinones are derivatized via both 1,4- and 1,6-addition to the ring (in which the latter is preferred) and also by addition to their side-chain carbons.[60]

(A) Synthesis and Characterization of 13_{red}. To definitively assign LTQ as the product of a 1,4-addition of lysine to tyrosine, we synthesized the alternative 1,6-addition product ($\mathbf{13}_{red}$) starting from 5-nitrovaniline in seven steps. Details of the synthesis are given in the Supporting Information. $\mathbf{13}_{red}$ has an absorption maximum at 266 nm at pH 7.2 which is 34 nm blue shifted compared to $\mathbf{1}_{red}$ (Figure 7a). $\mathbf{13}_{red}$ undergoes air oxidation, but the product is unstable. To obtain a clean UV−vis spectrum of the oxidized product of $\mathbf{13}_{red}$, the reaction was carried out in the presence of $NaIO_4$, where the oxidation of $\mathbf{13}_{red}$ was completed within 2 s. The oxidized product has a λ_{max} at 476 nm and approximately 740 nm (Figure 7b), but it was very unstable and underwent bleaching to yield a featureless spectrum within 10 min (Figure 7a).

Nonetheless, it was possible to obtain a quasi-reversible cyclic voltammogram ($\Delta E_p = 28$ mV) of the transient oxidized form (by air oxidation) of $\mathbf{13}_{red}$, yielding a midpoint potential of −0.106 V vs SCE (Figure 7c). The same value of E_m is measured using $\mathbf{13}_{red}$ as a starting product, suggesting that the oxidized product is the quinone (data not shown). This value is about 80 mV positive when compared to $\mathbf{1}_{ox}$. The instability of $\mathbf{13}_{ox}$ may only be applicable to solution chemistry, and such an adduct could be stabilized in the enzyme active site. However, the λ_{max} of $\mathbf{13}_{ox}$ is quite different from $\mathbf{1}_{ox}$, confirming the assignment of LTQ as the 1,4-addition product. Due to the instability of $\mathbf{13}_{ox}$, it was not possible to further characterize this analogue of LTQ.

(B) Formation of 3_{ox} from 4-Ethylphenol and *N*-Methyl-*n*-butylamine. To understand further how LTQ is formed from a tyrosine and a lysine residue in the active site of LOX, reactions were studied between amines and phenols or catechols in the presence of tyrosinase or $NaIO_4$ as an oxidant. This methodology is based on an earlier study where a number of amino acid cross-linked quinones were generated in situ by a reaction with catechols in the presence of tyrosinase.[61,62]

When 4-ethylphenol, a model compound for a tyrosine residue, is oxidized in the presence of tyrosinase and *N*-methyl-*n*-butylamine, $\mathbf{3}_{ox}$ is formed as the sole product (identified and quantitated by its UV−vis spectrum; Figure 8a). Tyrosinase catalyzes the hydroxylation of phenol to catechol and the oxidation of catechol to the *o*-quinone. The *o*-quinone reacts with the amine and, in the absence of amine, accumulates and gradually decomposes. Clearly, the reaction between the *o*-quinone and *N*-methyl-*n*-butylamine is rapid as only $\mathbf{3}_{ox}$ is detected when the amine is present, indicating a strong preference for 1,4-addition. When 4-ethylcatechol was used in place of 4-ethylphenol, the final product was similar to $\mathbf{3}_{ox}$; however, the spectrum of the final reaction mixture showed small differences (Figure 8b), suggesting that this reaction was not quite as clean. A similar result was obtained using $NaIO_4$ in place of tyrosinase with 4-ethylcatechol and *N*-methyl-*n*-butylamine. We suggest that the best way to prepare $\mathbf{3}_{ox}$ in situ is to start from 4-ethylphenol and to use tyrosinase as a catalyst for oxidation.

In contrast to *N*-methyl-*n*-butylamine, when *n*-butylamine was used as the nucleophile, the reaction was not clean, and multiple products were suggested by the UV−vis and NMR spectra (data not shown). $\mathbf{1}_{ox}$, if formed, is not the only product, concomitant with the expectation that the *o*-quinone would react in multiple

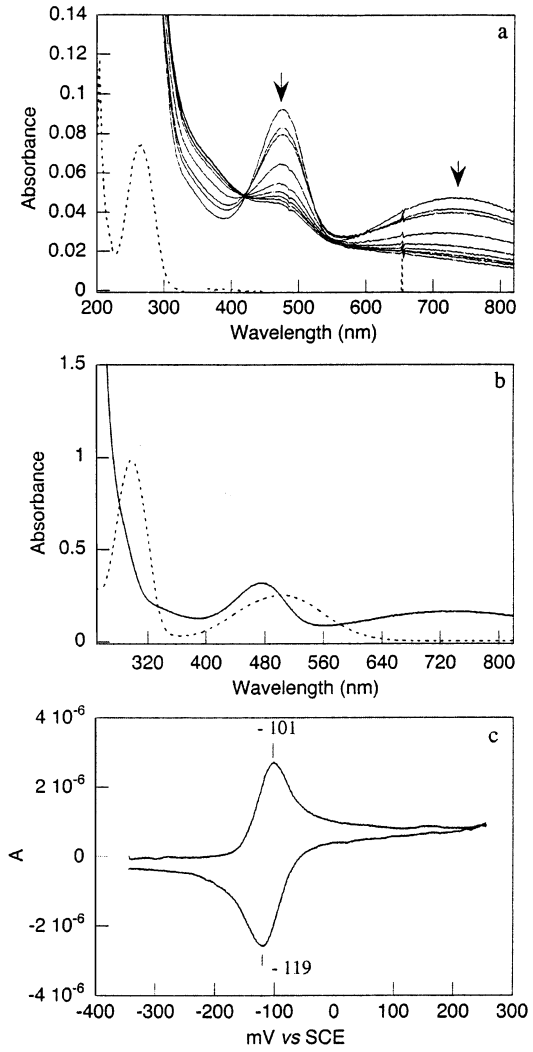

Figure 7. (a) UV−vis spectrum of $\mathbf{13}_{red}$ at pH 6.7 (- - -). Offset: Slow decomposition of $\mathbf{13}_{ox}$ following $NaIO_4$ oxidation of $\mathbf{13}_{red}$ as followed by the bleaching at 476 and 730 nm (2 s, 13 s, 30 s, 1 min, 2 min, 3 min, 5 min, 10 min). (b) Comparison of UV−vis spectra of $\mathbf{13}_{ox}$ (—) and $\mathbf{1}_{ox}$ (- - -). All spectra are for 0.1 mM of the appropriate model compound in 0.1 M potassium phosphate (pH = 6.7, I = 0.3 with KCl). (c) Cyclic voltammogram of $\mathbf{13}_{ox}$ at pH 6.7 at a scan speed of 100 mV s^{-1}. $\mathbf{13}_{ox}$ was in situ generated from air oxidation of $\mathbf{13}_{red}$. The direction of the scan is from positive to negative. Background (buffer) was subtracted.

(56) Waite, J. H. *Comp. Biochem. Physiol. B* **1990**, *97*, 19−29.
(57) Burzio, L. A.; Waite, J. H. *Biochemistry* **2000**, *39*, 11147−11153.
(58) Sugumaran, M. *Bioorg. Chem.* **1987**, *15*, 194.
(59) Akiyama, N.; Hijikata, M.; Kobayashi, A.; Yamori, T.; Tsuruo, T.; Natori, S. *Anticancer Res.* **2000**, *20*, 357−362.
(60) Christensen, A. M.; Schaefer, J.; Kramer, K. J.; Morgan, T. D.; Hopkins, T. L. *J. Am. Chem. Soc.* **1991**, *113*, 6799−6802.
(61) Mason, H. S.; Peterson, E. W. *Biochim. Biophys. Acta* **1965**, *111*, 134−146.
(62) Rzepecki, L. M.; Waite, J. H. *Anal. Biochem.* **1989**, *179*, 375−381.

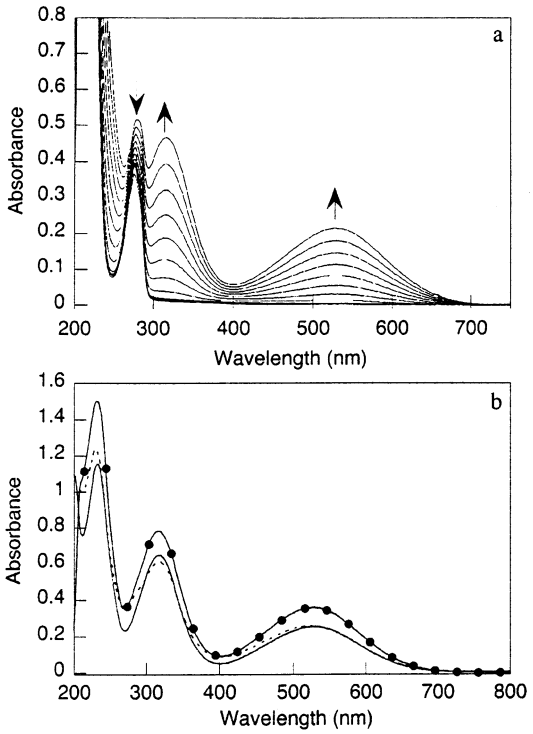

Figure 8. (a) Formation of $\mathbf{3}_{ox}$ from the reaction of *N*-methyl-*n*-butylamine and 4-ethylphenol catalyzed by mushroom tyrosinase. (b) Comparison of UV−vis spectra of authentic $\mathbf{3}_{ox}$ (—) with species formed from the oxidation of 4-ethylphenol (●) or 4-ethylcatechol (- - -) in the presence of *N*-methyl-*n*-butylamine. [4-Ethylphenol] = 2×10^{-4} M, [4-ethylcatechol] = 2×10^{-4} M, [*N*-methyl-*n*-butylamine] = 2×10^{-2} M, and [mushroom tyrosinase] = 0.2 μg/mL, in potassium phosphate buffer, pH 7.2.

ways with primary amines (1,2-, 1,4-, and 1,6-addition). *tert*-Butylamine did not yield any addition product, and isopropylamine reacted slowly and gave results similar to those of *n*-butylamine. In this particular model system, it is necessary to use *N*-methyl-*n*-butylamine to prevent the formation of a Schiff base (1,2-addition product).

These results suggest that the specific 1,4-cross-linking of tyrosine with the ϵ-amino group of lysine at the active site of LOX will be carefully controlled to prevent undesired products. The tyrosine-derived dopaquinone intermediate is generally accepted to be the precursor of the TPQ cofactor. To control the selectivity of nucleophilic attack, it is likely that the precursor protein is fully folded with the correct positioning of the lysyl side chain, prior to the initiation of oxidative chemistry on the precursor tyrosine. This will prevent unwanted chemistry involving the *o*-quinone intermediate. An analogous situation exists for the final step in the biogenesis of the TPQ cofactor, i.e., a Michael addition of hydroxide (water) to a dopaquinone intermediate. In aqueous solution, at neutral pH, the *o*-quinone does not undergo this reaction at an appreciable rate but, instead, slowly decomposes over the course of 3 h, with only trace amounts of TPQ (data not shown). Similar results have been observed for other 4-alkyl-1,2-benzoquinones which are resistant to hydration.[67] It has been shown that the precursor, the Cu^{2+}-free/Tyr-containing form of CAOs, folds in an identical manner to the mature protein (Cu^{2+}/TPQ form)[35,63] and that the biogenesis of TPQ is initiated upon addition of metal ion.[35,64,65] Cu^{2+} is proposed to play a key role in this step, providing an electrophilic center for the activation of tyrosine toward O_2[66] and for the reduction of the pK_a of the nucleophilic water that generates TPQ from dopaquinone.[33,36,67]

Conclusions

The synthesis of a model compound ($\mathbf{1}_{ox}$) for the LTQ cofactor of LOX together with a number of homologues has been presented. The characterization of these compounds, including their spectroscopic, acid−base, and redox properties, provides the groundwork for future studies of both LOX and its isozymes, as well as models of these physiologically important enzymes. The UV−vis spectroscopic properties of the phenylhydrazine adduct of $\mathbf{1}_{ox}$ and **4**, **2**, and **11** respectively, have been compared. The spectrum of **2** is similar to that of **11** at high pH, whereas low pH titrations indicate a different ionization for **2**; in this manner, the low-pH UV−visible spectral shift of **2** that is absent in **11** provides a means of distinguishing the LTQ cofactor from TPQ. Synthesis and characterization of a 1,6-adduct between dopaquinone and butylamine (**13**) confirm the assignment of LTQ as a 1,4-addition product. The non-specificity of primary amine addition to dopaquinone in solution suggests that the protein environment plays a key role in directing the nucleophilic addition of the ϵ-amino group of a lysyl side chain toward the correct position of the putative *o*-quinone intermediate in LTQ biogenesis. Further studies will focus on developing a model system to study the amine oxidation and reaction with LOX inhibitors.

Acknowledgment. We thank Dr. Graham Ball for acquiring 2D NMR spectra and Prof. Marcin Majda for allowing use of the BAS 100A electrochemical analyzer. M.M. also thanks Dr. Julian Limburg for critical reading of the manuscript. Supported by a grant from the NIH (GM39296 to J.P.K.).

Supporting Information Available: The experimental details of the synthesis of $\mathbf{13}_{red}$ and the NMR characterization of **2** and **10**. This material is available free of charge via the Internet at http://pubs.acs.org.

JA0214274

(63) Chen, Z.; Schwartz, B.; Williams, N. K.; Li, R.; Klinman, J. P.; Mathews, F. S. *Biochemistry* **2000**, *39*, 9709−9717.
(64) Matsuzaki, R.; Fukui, T.; Sato, H.; Ozaki, Y.; Tanizawa, K. *FEBS Lett.* **1994**, *351*, 360−364.
(65) Cai, D. Y.; Klinman, J. P. *J. Biol. Chem.* **1994**, *269*, 32039−32042.
(66) Schwartz, B.; Dove, J. E.; Klinman, J. P. *Biochemistry* **2000**, *39*, 3699−3707.
(67) Mandal, S.; Lee, Y.; Purdy, M. M.; Sayre, L. M. *J. Am. Chem. Soc.* **2000**, *122*, 3574−3584.